

Adjusted chi-square test for degree-corrected block models

Linfan Zhang and Arash A. Amini

January 1, 2021

Abstract

We propose a goodness-of-fit test for degree-corrected stochastic block models (DCSBM). The test is based on an adjusted chi-square statistic for measuring equality of means among groups of n multinomial distributions with d_1, \dots, d_n observations. In the context of network models, the number of multinomials, n , grows much faster than the number of observations, d_i , hence the setting deviates from classical asymptotics. We show that a simple adjustment allows the statistic to converge in distribution, under null, as long as the harmonic mean of $\{d_i\}$ grows to infinity. This result applies to large sparse networks where the role of d_i is played by the degree of node i . Our distributional results are nonasymptotic, with explicit constants, providing finite-sample bounds on the Kolmogorov-Smirnov distance to the target distribution. When applied sequentially, the test can also be used to determine the number of communities. The test operates on a (row) compressed version of the adjacency matrix, conditional on the degrees, and as a result is highly scalable to large sparse networks. We incorporate a novel idea of compressing the columns based on a $(K+1)$ -community assignment when testing for K communities. This approach increases the power in sequential applications without sacrificing computational efficiency, and we prove its consistency in recovering the number of communities. Since the test statistic does not rely on a specific alternative, its utility goes beyond sequential testing and can be used to simultaneously test against a wide range of alternatives outside the DCSBM family. The test can also be easily applied to Poisson count arrays in clustering or biclustering applications, as well as bipartite and directed networks. We show the effectiveness of the approach by extensive numerical experiments with simulated and real data. In particular, applying the test to the Facebook-100 dataset, a collection of one hundred social networks, we find that a DCSBM with a small number of communities (say < 25) is far from a good fit in almost all cases. Despite the lack of fit, we show that the statistic itself can be used as an effective tool for exploring community structure, allowing us to construct a community profile for each network.

1 Introduction

Network analysis has become an increasingly prominent part of data analysis as the developments in the age of the internet and in various sciences, especially life and social sciences, have produced a substantial collection of network data. Given a network, it is of interest to understand its structure, which is often done by finding communities or clusters. Probabilistic network models such as the Stochastic Block Model (SBM) [HLL83] and its variant the Degree-Corrected Stochastic Block Model (DCSBM) [KN11] are commonly used to recover the community structure from network data. Both models use a latent variable, the node label, to categorize nodes in a network into different communities. In the SBM, the probability of an

edge formation between two nodes depends on the communities they belong to. The DCSBM incorporates an additional propensity parameter to determine the edge probability, allowing heterogeneous node degrees within a community.

The SBM and its degree-corrected variant have been the subject of intense study in recent years and numerous methods have been developed for fitting them. A very incomplete list includes modularity maximization [NG04; BC09], likelihood-based approaches such as the profile likelihood [BC09; ZLZ12], the pseudo-likelihood [Ami+13] and the variational likelihood [DPR08; Bic+13; ZZ20], spectral methods based on the adjacency matrix [RCY11; CCT12; QR13; Fis+13; YP14; LR15; CRV15; JY16; ABH16; ZA19], the non-backtracking matrix [Krz+13] and the Bethe-Hessian matrix [SKZ14], semidefinite relaxations [ABH16; AL18; LCX18; FC19], local refinements [MNS16b; Gao+17; Gao+18; LZ17; ZA20b], message-passing algorithms [Dec+11; ZM14; AS15; MNS16a] and Bayesian approaches [SN97; HW08; MS12; Suw+16; PV18; PAL19]. Many of these methods are based on the assumption that the number of communities K is given and most come with consistency guarantees, when the data is generated from the corresponding model with K communities. We refer to [Abb18] for a review of the theoretical limits of community detection in SBMs.

On the other hand, how well these network models fit the data, the so-called goodness-of-fit question, is studied comparatively much less. Prominent work in this area include the graphical approach of [HGH08] for general network models, and the recent work of Bickel and Sarkar [BS16] and its extension by Lei [Lei16], on a spectral goodness-of-fit test for the SBM. Developing goodness-of-fit tests specifically for the DCSBM is more challenging and to the best of our knowledge has not been considered so far, except for the work of Karwa et al. [Kar+16] on the related β -SBM. A related problem is that of model selection, that is, determining the number of communities assuming that the network is generated from some SBM (or DCSBM). The model selection problem has been studied more extensively and we provide an overview of the literature in Section 1.1.

Compared to model selection, goodness-of-fit testing is a more general problem. When applied sequentially, such tests can also be used for model selection. However, their utility goes beyond model selection and they can be used to test against a wide range of alternatives. They also provide a quantitative and baseline-normalized measure of how well the model fits in various situations. On the other hand, the ability to simultaneously test against many alternatives can be considered a weakness. To quote L. Breiman [Bre01]:

“Work by Bickel, Ritov and Stoker (2001) [BRS06] shows that goodness-of-fit tests have very little power unless the direction of the alternative is precisely specified. The implication is that omnibus goodness-of-fit tests, which test in many directions simultaneously, have little power, and will not reject until the lack of fit is extreme.”

In our experiments, we have found the opposite to be true for current network models. It is possible to construct powerful tests, without specifying the direction of the alternative, for one of the most established family of network models. For example, we empirically demonstrate that the tests we develop for DCSBM are extremely powerful against a latent-variable community-structured model outside the DCSBM family (cf. Section 5.2.2). Moreover, for the majority of the real networks that we tested, the null hypothesis of a DCSBM with small number of communities is strongly rejected (cf. Section 5.3). This is all the more surprising given that the DCSBM is considered the state-of-the-art in modeling real community-structured networks.

In this paper, we propose the adjusted chi-square test for measuring the goodness-of-fit of a DCSBM. The idea is as follows: Given a set of labels, we compress the adjacency matrix by summing the rows over the communities specified by the labels. Under a DCSBM, the rows of the compressed matrix will have a multinomial distribution, conditional on the node degrees d_i (i.e., the row sums). Rows in the same (row) community will have the same multinomial parameter. Thus, the problem reduces to that of testing whether groups of multinomials have equal means. The challenge is that the number of multinomials in each group is proportional to n , the total number of nodes, which grows to infinity fast, while the number of observations in each multinomial, d_i , grows much slower. We study this general multi-group testing problem in Section 2.1 and show that under mild conditions, as long as the harmonic mean $h(d_1, \dots, d_n)$ goes to infinity, an adjusted version of the classical chi-square statistic has standard normal distribution under the null hypothesis.

We then develop these ideas in the context of networks and show that given a (strongly) consistent set of labels, by using a subsampling scheme, the same conclusion about the null distribution can be extended to the (S)NAC, the (subsampled) network adjusted chi-square statistic. NAC is, in fact, a family of tests, depending on what labels one uses for row compression. Using $(K + 1)$ -community column labels for compression, and K -community row labels when testing equality of multinomials, we obtain a powerful test in sequential applications. We refer to this variant as SNAC+ and, in Section 4.1, study its sequential consistency in determining the number of communities. We also develop bootstrapped versions of the tests which are more robust in practice and can be applied even when the null distribution of the test statistic is difficult to compute. Moreover, we introduce a smoothing idea that can further increase the robustness of sequential model selection.

Our theoretical results are non-asymptotic, controlling the Kolmogorov distance of the distribution of the test statistic to the target, with explicit constants. The results are valid in the regime where the expected average degree of the network, λ , scales as $\gtrsim \log n$, hence applicable in the same sparsity regime where strong consistency is possible for DCSBMs. From a computational standpoint, evaluating the statistic is highly scalable, with an expected computational overhead of $O(n(\lambda + K))$ over the cost of applying the community detection algorithm. To test a sequence of DCSBMs with $K = K_1, \dots, K_2$, the test requires an application of a community detection algorithm at most $K_2 - K_1 + 2$ times.

We show the effectiveness of these ideas with extensive experiments on simulated and real networks. The code for these experiments is available at [ZA20a]. In particular, we apply the test to the Facebook-100 dataset [Tra+11; TMP12], a collection of one hundred social networks, and find that a DCSBM (or SBM) with a small number of communities (say < 25) is far from a good fit in almost all cases. Despite the lack of fit, we show that the statistic itself can be used as an effective tool for exploring communities, due to its high sensitivity to block structure. Coupled with the smoothing idea, SNAC+ allows us to construct a *community profile* for each network, regardless of whether DCSBM is a good fit.

1.1 Related work

Various methods have been developed to address the model selection problem in the SBM and DCSBM. The popular Bayesian information criterion (BIC) has been adapted to the network setting in [Yan16; WB17; Hu+19]. Likelihood ratio tests have been developed for comparing two block models in [Yan+14a; WB17; YFS18; MSZ18]. Bayesian approaches,

though computationally intensive, can estimate the structure and the number of communities simultaneously. Ideas include the use of Dirichlet process prior [PAL19] and mixture of mixture priors [NR16; Rio+17; GBP19]. Cross-validation, another widely used idea for model selection, has too been adapted to network settings [KK17; CL18; LLZ20]. A leave-one-out scheme has been used in [KK17] with the posterior predictive density of an edge, under the SBM, as the loss function. Chen and Lei [CL18] use a node-pair splitting idea, while [LLZ20] uses edge sampling followed by low-rank matrix completion, an approach that can be applied to any low-rank network model. A spectral approach to determining the number of communities in the SBM is explored in [LL15], based on counting the nonnegative eigenvalues of the non-backtracking and Bethe Hessian matrices. The approach of [LL15] can be extended to other low-rank structured models such as DCSBM. Semidefinite programming have been shown in [YSC18] to be capable of performing label recovery and model selection in one shot. Modularity maximization can also perform the two tasks simultaneously [NG04].

Comparatively, the goodness-of-fit problem has been explored much less. The pioneering work of [HGH08] graphically compares certain network statistics (such as degree distribution) between the observed network and a collection of networks simulated from the fitted model. This approach is quite general and can be applied to any network model, though its graphical nature makes it somewhat qualitative. The Monte Carlo simulation procedures in [HGH08] have also been further exploited in other works [LC13; OFDR19] to test the goodness-of-fit of graph models. Among them, we note that Karwa et al. [Kar+16] develops a chi-square test for SBM and uses Markov Chain Monte Carlo sampling to approximate its exact p -value. We make a detailed comparison with [Kar+16] in Section 4.2. For SBMs, a spectral goodness-of-fit was developed in [BS16] for the case of $K = 2$ communities and subsequently extended to general K in [Lei16]. The test is based on the largest eigenvalue of a standardized residual adjacency matrix (cf. Section 5.1 for more details). Using results from random matrix theory [EYY12; LY+14], this eigenvalue has an asymptotic Tracy-Widom distribution under the null, a result that can be used to set the critical threshold. Although, we can apply the same ideas in the DCSBM setting, the null distribution result does not hold, due to the uncertainty in estimating the node connection propensity parameters. Whether a rigorous spectral goodness-of-fit test of this form exists for DCSBM is not clear.

The rest of the paper is organized as follows: Section 2 introduces the adjusted chi-square test and its multi-group extension and establishes its null limiting distribution. Section 3 introduces NAC family of tests. Section 4 provides the analysis of SNAC+, under a sparse DCSBM, and establishes its null limiting distribution and consistency in sequential selection. Section 5 demonstrates the competitive performance of NAC tests, as a model selection method, compared other state-of-the-art approaches. In Section 5.3, we illustrate how SNAC+ can be used to assess the goodness-of-fit for an ensemble of real networks, namely the Facebook-100 dataset. Section 5.4 discusses how smoothed SNAC+ can be used to build community profiles of real networks. We conclude with the proofs of the main results in Section 6.

2 Adjusted chi-square test

We start by developing a general test for the equality of the parameters among groups of multinomial observations. To set the ideas, we first consider the case of a single group and show how the classical chi-square test can be adjusted to accommodate a growing number of

multinomials. We then discuss the multi-group extension and provide quantitative bounds for the null distribution of the test statistic in this general setting.

2.1 Single-group case

Let \mathcal{P}_L be the probability simplex in \mathbb{R}^L , and consider the following problem: We have

$$X_i \sim \text{Mult}(d_i, p^{(i)}), \quad i = 1, \dots, n, \quad (1)$$

independently, where $X_i = (X_{i\ell}) \in \mathbb{N}^L$ and $p^{(i)} \in \mathcal{P}_L$, and we would like to test the null hypothesis

$$H_0 : p^{(1)} = p^{(2)} = \dots = p^{(n)} = p. \quad (2)$$

Let $\psi(x, y) := (x - y)^2/y$. The chi-square statistic for testing this hypothesis is

$$\widehat{Y}^{(n,d)} := \sum_{i=1}^n \sum_{\ell=1}^L \psi(X_{i\ell}, d_i \widehat{p}_\ell), \quad \text{where} \quad \widehat{p}_\ell = \frac{\sum_{i=1}^n X_{i\ell}}{\sum_{i=1}^n d_i}, \quad \ell \in [L].$$

Here, $\widehat{p} = (\widehat{p}_\ell) \in \mathcal{P}_L$ is the pooled estimate of p under the null, and $d = (d_1, \dots, d_n)$. We are also using the shorthand notation $[L] := \{1, \dots, L\}$.

Standard asymptotic theory gives the following (cf. Chapter 17 in [Vaa98]): If n is fixed and $d_{\min} := \min_i d_i \rightarrow \infty$, then,

$$\widehat{Y}^{(n,d)} \rightsquigarrow \chi_{(n-1)(L-1)}^2, \quad \text{under } H_0. \quad (3)$$

A heuristic for the degrees of freedom of the limiting χ^2 distribution can be given by counting parameters. In the unrestricted model, we have a total of $n(L-1)$ free parameters among $p^{(1)}, \dots, p^{(n)}$, while under the restricted null model, we only have $L-1$ free parameters. The difference gives the degrees of freedom of the limit.

The setting we are interested in, however, is the opposite of the classical setting. We would like to use the statistic when $n \rightarrow \infty$, while d_{\min} is fixed or grows slowly with n . Assuming that n is large enough so that $(n-1)(L-1) \approx n(L-1)$, (3) suggests that we can approximate $\widehat{Y}^{(n,d)}$ in distribution by the sum of n independent χ_{L-1}^2 variables, i.e., $\widehat{Y}^{(n,d)} \stackrel{d}{\approx} R_n := \sum_{i=1}^n \xi_i$ where ξ_i are i.i.d. draws from χ_{L-1}^2 . Moreover, the central limit theorem suggests that the standardized version of R_n has a distribution close to a standard normal.

Based on the above heuristic argument, we propose the following adjusted test statistic:

$$\widehat{T}_n = \frac{1}{\sqrt{2}} \left(\frac{\widehat{Y}^{(n,d)}}{\gamma_n} - \gamma_n \right), \quad \text{where } \gamma_n = \sqrt{n(L-1)}. \quad (4)$$

Note that γ_n^2 is the expectation of R_n and $\sqrt{2}\gamma_n$ is its standard deviation. We refer to (4) as the *adjusted chi-square* (AC) statistic.

2.2 Multi-group extension

Before proceeding, let us introduce an extension of the testing problem (2) to groups of observations. This extension is needed for the network applications. Consider model (1) and assume that each observation is assigned to one of the K known groups, denoted as $[K] = \{1, \dots, K\}$. Let $g_i \in [K]$ be the group assignment of observation i and let $\mathcal{G}_k = \{i \in [n] : g_i = k\}$ be the k th group. We would like to test the null hypothesis that all the observations in the same group have the same parameter vector, that is,

$$H_0 : p^{(i)} = p_{k*}, \forall i \in \mathcal{G}_k, k \in [K], \quad (5)$$

where for each $k \in [K]$, $p_{k*} = (p_{k\ell})_{\ell \in [L]} \in \mathcal{P}_L$. Consider the following extension of the chi-square statistic

$$\widehat{Y}^{(n,d)} = \sum_{k=1}^K \sum_{i \in \mathcal{G}_k} \sum_{\ell=1}^L \psi(X_{i\ell}, d_i \widehat{p}_{k\ell}) \quad \text{where} \quad \widehat{p}_{k\ell} = \frac{\sum_{i \in \mathcal{G}_k} X_{i\ell}}{\sum_{i \in \mathcal{G}_k} d_i}, \ell \in [L]. \quad (6)$$

Alternatively, we can write $\widehat{Y}^{(n,d)} = \sum_{i=1}^n \sum_{\ell=1}^L \psi(X_{i\ell}, d_i \widehat{p}_{g_i\ell})$. The corresponding adjusted chi-square statistic, \widehat{T}_n , is still given by (4) based the new definition of $\widehat{Y}^{(n,d)}$. We also let $Y^{(n,d)}$ be the idealized version of $\widehat{Y}^{(n,d)}$ with $\widehat{p}_{k\ell}$ replaced with $p_{k\ell}$, and let T_n be the adjusted chi-square statistic based on $Y^{(n,d)}$, that is,

$$T_n = \frac{1}{\sqrt{2}} \left(\frac{Y^{(n,d)}}{\gamma_n} - \gamma_n \right). \quad (7)$$

We are interested in understanding under what conditions \widehat{T}_n has an approximately standard normal null distribution. This question is nontrivial, since we would like to allow $\{d_i\}$ as well as groups sizes $|\mathcal{G}_k|, k \in [K]$ to potentially vary with n . We give a precise answer to this question by quantifying the Kolomogorv distance between the distribution of \widehat{T}_n and that of a standard normal variable Z , for any choice of $\{d_i\}$ and $\{|\mathcal{G}_k|\}$ that satisfy a mild set of conditions.

Recall that for two random variables X and Y , the Kolomogrov distance between their distributions is defined as

$$d_K(X, Y) := \sup_{t \in \mathbb{R}} |\mathbb{P}(X \leq t) - \mathbb{P}(Y \leq t)|. \quad (8)$$

For a vector $d = (d_1, \dots, d_n)$, we write $h(d) = (n^{-1} \sum_{i=1}^n d_i^{-1})^{-1}$ for the harmonic mean of its elements, and $d_{\text{av}} = n^{-1} \sum_{i=1}^n d_i$ for the arithmetic mean. Since d has positive elements, $d_{\text{av}} \geq h(d) \geq d_{\min} := \min_i d_i$. Let $\pi_k = |\mathcal{G}_k|/n$ and write $d_{\text{av}}^{(k)} = \frac{1}{|\mathcal{G}_k|} \sum_{i \in \mathcal{G}_k} d_i$ for the arithmetic average of $\{d_i\}$ within group \mathcal{G}_k , and define

$$\omega_n := \min_k \pi_k d_{\text{av}}^{(k)}. \quad (9)$$

The following result formalizes the heuristic argument above, by providing a quantitative finite-sample bound on the Kolomogrov distances of T_n and \widehat{T}_n to a standard normal variable:

Theorem 1. Let $X_i \sim \text{Mult}(d_i, p_{k*})$, $i \in \mathcal{G}_k, k \in [K]$ be n independent L -dimensional multinomial variables, with probability vectors $p_{k*} = (p_{k\ell})$, and assume that $\min\{h(d), L\} \geq 2$. Let T_n be as in (7), $Z \sim N(0, 1)$ and $\underline{p} = \min_{k,\ell} p_{k\ell}$. Then, under the null hypothesis (5), for all $n \geq 1$,

$$d_K(T_n, Z) \leq \frac{C_{1,p}}{\sqrt{Ln}} + \frac{C_{2,p}}{h(d)} \quad (10)$$

where $C_{1,p} = 55/p^4$ and $C_{2,p} = (\pi e)^{-1/2} \max\{1, \underline{p}^{-1} - L - 1\}$. Moreover, assuming $\omega_n \geq L$ and $\log(K\omega_n)/\omega_n \leq (\underline{p}/8)^2 n$, we have

$$d_K(\widehat{T}_n, Z) \leq d_K(T_n, Z) + \frac{\sqrt{L}}{\underline{p}} \left(\sqrt{\frac{32 \log(K\omega_n)}{\omega_n}} + \frac{12K \log(K\omega_n)}{\sqrt{n}} \right). \quad (11)$$

Note that we always have $\underline{p}^{-1} \geq L$ since the elements of p_{k*} are nonnegative and sum to one. In the proof of Theorem 1, we will show that $\mathbb{E}[Y^{(n,d)}] = \gamma_n^2$. But the standard deviation $v_n(\underline{p}) := \sqrt{\text{var}[Y^{(n,d)}]}$ has a more complicated form and is not equal to $\sqrt{2}\gamma_n$ in general. The proof gives an explicit expression for this variance, and we could have alternatively defined \widehat{T}_n by dividing by $v_n(\widehat{\underline{p}})$ instead of $\sqrt{2}\gamma_n$. Nevertheless, Theorem 1 shows that we do not lose much by using the simpler standardization by $\sqrt{2}\gamma_n$.

The condition $h(d) \geq 2$ holds when $d_i \geq 2$ for all i . Since for networks, d_i will be the degree of node i , this condition is very mild. In general, for T_n to converge in distribution to the standard normal, we need $n \rightarrow \infty$ and $h(d) \rightarrow \infty$. For \widehat{T}_n to converge to the normal distribution, we further need $\omega_n \rightarrow \infty$ and $K \log(K\omega_n) = o(\sqrt{n})$. Note that $\log(K\omega_n)/\omega_n \leq (\underline{p}/8)^2 n$ is satisfied for large n , as long as \underline{p} is bounded away from zero. When there is only one single group, the requirements are $d_{\text{av}} \rightarrow \infty$, which is implied by $h(d) \rightarrow \infty$, and $\log(d_{\text{av}}) = o(\sqrt{n})$.

As we will see, in network applications, typically K , L and \underline{p} are of constant order, $\omega_n \log \omega_n \lesssim n$ and the degrees $\{d_i\}$ are of the same order, hence $h(d) \asymp \omega_n$. In such settings, we obtain the rate of convergence $d_K(\widehat{T}_n, Z) = O(\sqrt{\log \omega_n / \omega_n})$.

3 Network AC test

We are now ready to apply the AC test to DCSBMs. Let $A_{n \times n}$ be the adjacency matrix of a random network on n nodes. A DCSBM with connectivity matrix $B \in [0, 1]^{K \times K}$, node label vector $z = (z_i) \in [K]^n$ and connection propensity vector $\theta = (\theta_i) \in \mathbb{R}_+^n$, assumes the following structure for the mean of A ,

$$\mathbb{E}[A_{ij} | z] = \theta_i \theta_j B_{z_i z_j}, \quad \forall i \neq j. \quad (12)$$

One further assumes that A is symmetric and the entries $A_{ij}, i < j$ are drawn independently, while $A_{ii} = 0$ for all i . Common choices for the distribution of each element, A_{ij} , are Bernoulli and Poisson. In this paper, unless otherwise stated, we assume the Poisson distribution for derivations, following the original DCSBM paper [KN11]. The Poisson assumption simplifies the arguments and provides computational advantages. We show in simulations that the tests so-derived work well in the Bernoulli case when the network is sparse. The SBM is a special case of (12) with $\theta_i = 1$ for all i .

3.1 NAC family of tests

The test can be performed on a general submatrix $A_{S_2 S_1} = (A_{i,j} : i \in S_2, j \in S_1)$ of the adjacency matrix, for $S_1, S_2 \subset [n]$. We present this general form, though one can assume $S_1 = S_2 = [n]$ on the first reading. Consider another label vector on S_1 , say $\hat{y} = (\hat{y}_j)_{j \in S_1} \in [L]^{S_1}$ —for some L that could be different from K . Let $R = (R_{k\ell}) \in \mathbb{R}_+^{K \times L}$ be the weighted confusion matrix between z_{S_2} and \hat{y} , given by

$$R_{k\ell} = \frac{1}{|S_1|} \sum_{j \in S_1} \theta_j \mathbf{1}\{z_j = k, \hat{y}_j = \ell\}. \quad (13)$$

Consider the column compression of $A_{S_2 S_1}$ w.r.t. \hat{y} , defined as $X = (X_{i\ell}) \in \mathbb{R}_+^{|S_2| \times L}$, with

$$X_{i\ell}(\hat{y}) = \sum_{j \in S_1} A_{ij} \mathbf{1}\{\hat{y}_j = \ell\}. \quad (14)$$

Assuming that \hat{y} is deterministic, we have

$$\mathbb{E}[X_{i\ell}(\hat{y})] = \sum_{j \in S_1} B_{z_i z_j} \theta_i \theta_j \mathbf{1}\{\hat{y}_j = \ell\} = \theta_i \sum_{k=1}^K B_{z_i k} \sum_{j \in S_1} \theta_j \mathbf{1}\{z_j = k, \hat{y}_j = \ell\} = |S_1| \theta_i (BR)_{z_i \ell}.$$

Let $d_i = \sum_{j \in S_1} A_{ij}$ be the degree of node i on S_1 . Under the Poisson model for A_{ij} , we have

$$X_{i*}(\hat{y}) \mid d_i \sim \text{Mult}(d_i, \rho_{z_i*}), \quad (15)$$

where ρ_{z_i*} denotes the z_i th row of $\rho = (\rho_{k\ell}) \in [0, 1]^{K \times L}$, defined as

$$\rho_{k\ell} = \frac{(BR)_{k\ell}}{\sum_{\ell'} (BR)_{k\ell'}}. \quad (16)$$

In other words, conditioned on the degree sequence $d = (d_i, i \in S_2)$, all the rows of X corresponding to z -community k , have multinomial distributions with probability vector ρ_{k*} . This observation allows us to apply the AC test developed in Section 2.2, to test whether all the rows with $z_i = k$, have the same multinomial distribution.

Motivated by the above discussion, we consider the following general test statistic. Consider two estimated label vectors $\hat{z} = (\hat{z}_i) \in [K]^n$ and $\hat{y} = (\hat{y}_i) \in [L]^{S_1}$. Let $\hat{C}_k = \{i \in [n] : \hat{z}_i = k\}$, $\hat{G}_k = \hat{C}_k \cap S_2$ and $\tilde{n} = |S_2|$. Consider the multi-group version of the AC statistic:

$$\hat{T}_n = \frac{1}{\sqrt{2}} \left(\frac{1}{\gamma_{\tilde{n}}} \sum_{k=1}^K \sum_{i \in \hat{G}_k} \sum_{\ell=1}^L \psi(X_{i\ell}(\hat{y}), d_i \hat{\rho}_{k\ell}) - \gamma_{\tilde{n}} \right) \quad (17)$$

where $\gamma_{\tilde{n}} = \sqrt{\tilde{n}(L-1)}$ and

$$\hat{\rho}_{k\ell} = \frac{\sum_{i \in \hat{G}_k} X_{i\ell}(\hat{y})}{\sum_{i \in \hat{G}_k} d_i}, \quad k \in [K], \ell \in [L]. \quad (18)$$

The above construction specifies a family of test statistics, depending on the choices of label vectors \hat{z} and \hat{y} . We specifically consider two members of this family, namely,

1. NAC: $\hat{y} = \hat{z}$ and \hat{z} is an estimated label vector with K communities,
2. NAC+: \hat{z} and \hat{y} are estimated label vectors with K and $L = K + 1$ communities.

The acronym NAC stands for Network Adjusted Chi-square. In both cases, K is the number of communities under null. Both versions can be used as goodness-of-fit tests for a DCSBM with a given number of communities. As will be shown in Theorem 3, NAC+ is especially powerful when determining the number of communities by sequential testing. We refer to the case where $S_1 = S_2 = [n]$, as the full version of (each) test.

Remark 1. The NAC family of tests are easily applicable to non-square and nonsymmetric adjacency matrices, with potentially unequal number of communities or clusters for the rows and columns. In particular, they can be used to test directed or bipartite DCSBMs or SBMs. In addition, they can be easily applied if the cluster structure of one side is known but not the other. For example, they can be used for model selection and goodness-of-fit testing in problems involving clustering and biclustering of (Poisson) count arrays, a common task in contemporary bioinformatics [AH10]. In this paper, we focus on the symmetric DCSBM for simplicity. All the results hold in the general nonsymmetric case as well, with suitable modifications.

3.2 Subsampled version

Consider the full version of the NAC+ test based on (17) with $S_1 = S_2 = [n]$. Although the critical region of this test can be set by simulation, there are two obstacles in determining the exact asymptotic null distribution. The main obstacle is that the label estimation procedures used for obtaining \hat{z} and \hat{y} often process the entire adjacency matrix. This means that $X_{i\ell}(\hat{y})$ is a sum of the entries of A over a subset that is statistically dependent on those entries, hence the resulting distribution could, in general, be complicated. The other difficulty is the symmetry of A which makes $X_{i*}(\hat{y})$ and $X_{j*}(\hat{y})$ (mildly) dependent through the shared element $A_{ij} = A_{ji}$, even when $\hat{y} = z$, the true label vector.

We now introduce a subsampled version of the test that circumvents the above obstacles. The idea is as follows:

1. Fit K communities to the whole network (i.e., entire A) to get labels $\hat{z} \in [K]^n$.
2. Choose a subset $S_1 \subset [n]$ by including each index $i \in [n]$, independently, with probability $1/2$. Let $S_2 = [n] \setminus S_1$ be the complement of S_1 .
3. Fit L communities to $A_{S_1 S_1} = (A_{ij} : i, j \in S_1)$, to learn the label vector \hat{y} on S_1 .
4. Perform the test on $A_{S_2 S_1}$ using row labels \hat{z}_{S_2} and column labels \hat{y} from Step 3.

We refer to the subsampled version of NAC as SNAC, and similarly for NAC+. In Section 4, we show that, under the null model, the distributions of the test statistics of SNAC and SNAC+ are close to a standard normal. Furthermore, SNAC+ is large when the model is underfitted, i.e., the presumed number of communities is smaller than that of the true model. Such properties allow us to use SNAC+ for assessing the goodness-of-fit of DCSBM or SBM to an observed network and to determine the number of clusters in community detection.

3.3 Bootstrap debiasing

We can use bootstrap to correct the deviation of the null distribution of the NAC+ statistic from the standard normal. The bias could result from two sources. Firstly, the NAC+ test is based on Poisson generation, so when applied to a Bernoulli network, its null distribution could shift from the standard normal. The second source is the label dependence issue, in the case of the full NAC+, as discussed in Section 3.2. Though the subsampled version of the test, SNAC+, removes the dependence, the full version is expected to have more power as it utilizes all the nodes in the network.

Given adjacency matrix A , the null hypothesis that the number of communities is K , and the test statistic $\hat{T} = \hat{T}(A)$, the bootstrap debiasing is performed as follows:

1. Fit a K -community SBM to A and get label estimates \hat{z} and connectivity matrix \hat{B} .
2. For $j = 1, \dots, J$, sample $A^{(j)} \sim \text{SBM}(\hat{z}, \hat{B})$ and evaluate the test statistic $\hat{T}^{(j)}$ based on $A^{(j)}$.
3. Construct the debiased statistic $\hat{T}^{(\text{boot})} = (\hat{T} - \hat{\mu}) / \hat{\sigma}$ where $\hat{\mu}$ and $\hat{\sigma}$ are the sample mean and the standard deviation of $\{\hat{T}^{(j)}\}_{j=1}^J$.

Note that we sample from SBM instead of DCSBM, since the estimator of θ could have a large variance. The test rejects for large values of $\hat{T}^{(\text{boot})}$ (or $|\hat{T}^{(\text{boot})}|$), with the threshold set, assuming that $\hat{T}^{(\text{boot})}$ has (approximately) a standard normal distribution under null. An alternative to debiasing is to use the empirical quantiles of $\{T^{(j)}\}$ to set the critical threshold. We, however, found that the debiasing approach performs better in practice. A similar idea is used in [Leil16] for the spectral test. As the simulations in Section 5 show, the debiasing has little effect on SNAC+ in practice, illustrating that the normal approximation is already good enough, without performing the bootstrap.

3.4 Model selection

As alluded to before, a goodness-of-fit test can also be used as a model selection method, through a process of sequential testing. In particular, we can use NAC and NAC+ to determine the number of communities when fitting DCSBM models.

The idea is to test the null hypothesis of K communities, starting with $K = K_{\min}$, which is usually taken to be 1, and increasing K to $K + 1$ if the null is rejected. The process is repeated until we can no longer reject the null or a preset maximum number of communities, K_{\max} , is reached. The value of K on which we stop is selected as the optimal number of communities. We refer to this procedure as *sequential testing from below*. There is also the possibility of starting at $K = K_{\max}$ and working backwards. Testing from below is, however, more advantageous, especially if one expects a small number of communities a priori.

The rejection thresholds for SNAC+ and SNAC can be determined based on the standard normal distribution. For NAC+, we need to apply the bootstrap debiasing of Section 3.3 before comparing the statistic with the threshold. Theorem 3 provides a theoretical guarantee for the consistency of the sequential testing from below, when SNAC+ is used. An empirical comparison of the model selection performance of this approach, with existing methods, is provided in Section 5.2.1.

4 Analysis of SNAC+

We now provide a theoretical analysis of SNAC+. We consider a DCSBM with K_0 true community, and the edge probability matrix $B = (\nu_n/n)B^0$ where ν_n is a scaling factor and B^0 satisfies

$$\min_{k,\ell} B_{k\ell}^0 \geq \tau_B \cdot \max_{k,\ell} B_{k\ell}^0. \quad (19)$$

Let $\mathcal{C}_k = \{i \in [n] : z_i = k\}$ be the true community k . We assume that

$$n_k := |\mathcal{C}_k| \geq \tau_{\mathcal{C}} n, \quad \theta_i \geq \tau_{\theta} \cdot \max_i \theta_i \quad (20)$$

for all $k \in [K_0]$ and $i \in [n]$. Here, $\tau_B, \tau_{\mathcal{C}}$ and τ_{θ} are in $(0, 1]$ and measure the deviation of the corresponding parameters from being balanced. To make ν_n identifiable, we further assume without loss of generality that $\|B^0\|_{\infty} := \max_{k,\ell} B_{k\ell}^0 = 1$ and $\|\theta\|_{\infty} := \max_i \theta_i = 1$.

We also require the community detection algorithm to recover the true communities well and does not produce extremely small communities when the presumed number of clusters is close to K_0 .

Assumption 1. *The community detection algorithm applied with K communities to the DCSBM described above, producing labels $\{\hat{z}_i\}$, satisfies:*

(a) δ_n -consistency: $\mathbb{P}(z = \hat{z}) \geq 1 - \delta_n$ when $K = K_0$.

(b) Stability: $|\{i : \hat{z}_i = k\}| \geq \tau_0 n$ for all $k \in [K]$, when $K \in \{1, \dots, K_0 - 1, K_0 + 1\}$.

We further assume that $n \mapsto \delta_n$ is nonincreasing.

The consistency of the algorithm allows us to focus on the event $\{\hat{z} = z\}$, under the null model, and the stability allows us to lower-bound ρ , defined in (16). Condition (a) in Assumption 1 is known as the strong consistency or exact recovery, and it is well-known that if $\nu_n \gtrsim \log n$, there are algorithms that can achieve it [Abb18]. Note that the growth rate of ν_n is roughly that of the expected average degree (EAD) of the network, assuming that B^0 , $\{n_k/n\}_k$ and the distribution of $\{\theta_i\}$ are roughly constant. Hence, assuming $\nu_n \gtrsim \log n$ imposes a mild restriction on the network, requiring the EAD to grow at least as $\log n$. The stability condition (b) is even milder and can be guaranteed by explicitly enforcing it in the algorithm. If the size of a recovered community is too small relative to n , we merge it with another community. Whether a specific community detection algorithm satisfies this condition automatically without explicit enforcement is an interesting research question.

To state further assumptions, we define the following constants:

$$c_1 := 0.4 \frac{\tau_{\mathcal{C}}}{K_0}, \quad C_1 := \tau_{\theta}^2 \tau_{\mathcal{C}} \min_h \|B_{h*}^0\|_1, \quad (21)$$

$$\tau_a := \tau_{\theta} \tau_B \tau_{\mathcal{C}}, \quad \tau_{\rho} := \tau_{\theta} \tau_B \tau_0. \quad (22)$$

Throughout, c_1 and C_1 will be the constants defined above. Other constants are denoted as C_2, C_3, \dots and c_2, c_3, \dots and could be different in each occurrence. We make the following scaling assumptions:

$$\frac{\nu_n}{\log n} \geq \frac{1000}{C_1} \quad \text{and} \quad \frac{n}{\log n} \geq \frac{400}{3C_1} \vee \frac{300}{\tau_{\mathcal{C}}}. \quad (23)$$

Our first result establishes the null distribution of SNAC+.

Theorem 2 (Null distribution). *Consider an $n \times n$ adjacency matrix A that is generated from a Poisson DCSBM with K_0 blocks, satisfying (19) and (20). Let \widehat{T}_n be the test statistic of SNAC+ applied with $K = K_0$ and $L = K_0 + 1$ and a community detection algorithm satisfying Assumption 1. Let $\alpha_n = \log((9/8)K_0^2\nu_n)$ and $\kappa_0 = \tau_\rho$ and assume in addition that $(C_1/6)\tau_C\nu_n \geq L \geq 2$ and $\alpha_n/\nu_n \leq (C_1/6)\tau_C(\kappa_0/8)^2n$ where C_1 is as defined in (21). Then,*

$$d_K(\widehat{T}_n, Z) \leq \frac{C_3}{\sqrt{Ln}} + \frac{C_4}{C_1\nu_n} + \frac{19\sqrt{L}}{\kappa_0} \left(\sqrt{\frac{\alpha_n}{C_1\tau_C\nu_n}} + \frac{K_0\alpha_n}{\sqrt{n}} \right) + 2\delta_n$$

where $C_3 = 7 + 87/\kappa_0^4$ and $C_4 = 4(\pi e)^{-1/2} \max\{1, \kappa_0^{-1} - L - 1\}$.

The same result holds for SNAC by redefining $\kappa_0 = (2/3)\tau_\rho$, $L = K_0$ and $C_3 = 14 + 87/\kappa_0^4$, and replacing $2\delta_n$ in the bound with $2\delta_n + \delta_{0.4n}$.

Assuming the common scaling $\log n \lesssim \nu_n \lesssim \sqrt{n}$, the dominant term in the bound is $\sqrt{\alpha_n/\nu_n}$, hence, under the null, we obtain

$$d_K(\widehat{T}_n, Z) \lesssim \sqrt{\frac{\log \nu_n}{\nu_n}} + \delta_n,$$

showing that \widehat{T}_n is asymptotically normal, and providing a rate of convergence for its normal approximation.

4.1 Consistency

Next, we consider the consistency of SNAC+ when applied in sequential testing from below, to determine the number of communities. In particular, we analyze its power in distinguishing the null hypothesis $H_0 : K = K_0$ from the alternative $H_1 : K < K_0$. Theorem 3 provides a lower bound on the growth rate of the test statistic \widehat{T} under the alternative.

Recall that \widehat{y} are labels derived for nodes S_1 based on $A_{S_1 S_1}$. Let parameters $\rho_{k\ell}$ be defined as in (16), and let

$$\omega_2 = \frac{1}{18}\tau_\theta^2\tau_a^2c_1^2 \min_{k,h \in [K_0]: k \neq h} \frac{1}{L} \|\rho_{k*} - \rho_{h*}\|_2^2. \quad (24)$$

Note that ω_2 is a random quantity due to the randomness in \widehat{y} .

Theorem 3 (Power). *Let A be an $n \times n$ adjacency matrix generated from a Poisson DCSBM with K_0 blocks that satisfies (19) and (20). Let \widehat{T}_n be the SNAC+ test statistic (17) formed as detailed in Section 3.2, with $K < K_0$ and $L = K + 1$ communities, and a community detection algorithm satisfying Assumption 1. Moreover, let $\underline{q} = \frac{2}{3}c_1\tau_\theta\tau_a\tau_\rho$ and $C_2 := c_1C_1/10$ and assume that $(\log n)/\nu_n \leq \frac{C_1}{64}\underline{q}^2$ and consider the event*

$$\Omega_n = \left\{ \max \left(\frac{1}{C_2\nu_n}, \frac{768}{\underline{q}^3} \sqrt{\frac{\log n}{C_1\nu_n}} \right) \leq \omega_2 \right\}. \quad (25)$$

Then, with probability at least $1 - 9Ln^{-1} - \mathbb{P}(\Omega_n^c)$,

$$\widehat{T}_n \geq C_2\omega_2\nu_n\sqrt{Ln}.$$

Quantity ω_2 that appears in Theorem 3 is random (via $\{\rho_{k\ell}\}$) and depends on the specific community detection algorithm used to form the test statistic. As discussed below, for any reasonable algorithm, under mild conditions on the connectivity matrix, we expect ω_2 to be of constant order as $n \rightarrow \infty$, i.e., $\omega_2 \asymp 1$. In particular, we expect to have $\mathbb{P}(\omega_2 \geq c_2) \rightarrow 1$ for some constant $c_2 > 0$, as $n \rightarrow \infty$. Then, we have $\mathbb{P}(\Omega_n^c) \rightarrow 0$, as long as $(\log n)/\nu_n \leq c_2$.

Under these assumptions, Theorem 2 shows that for a given $\alpha > 0$, $\widehat{T}_n \asymp 1$ with probability $1 - \alpha$ when $K = K_0$, while Theorem 3 guarantees that $\widehat{T}_n \gtrsim \nu_n \sqrt{n}$, w.h.p., when $K < K_0$. This shows that SNAC+ with a constant threshold or one that grows slower than $\nu_n \sqrt{n}$, leads to consistent model selection when applied sequentially from below (i.e., with $K < K_0$). In short, model selection consistency of SNAC+ only requires $(\log n)/\nu_n = O(1)$, that is, the expected degree should grow no slower than $\log n$.

The easiest way to see that ω_2 is, in general, bounded below, is to consider the hardest case in Theorem 3, that is, testing the null hypothesis $K = K_0 - 1$ against the alternative $K = K_0$. Since $L = K + 1 = K_0$ in this case, the estimated column labels \widehat{y} match the true labels z , under the exact recovery Assumption 1. Recalling the definition of the confusion matrix from (13), we obtain $R = \text{diag}(\widetilde{\pi}_k)$, where $\widetilde{\pi}_k = \frac{1}{|S_1|} \sum_{j \in S_1} \theta_j 1\{z_j = k\}$ for all $k \in [K_0]$. Then, $\rho_{k\ell} = B_{k\ell}^0 \widetilde{\pi}_\ell / (\sum_{\ell'} B_{k\ell'}^0 \widetilde{\pi}_{\ell'})$. Note that both B^0 and $\{\widetilde{\pi}_k\}$ are stable as $n \rightarrow \infty$. In particular, although the entries of B vanish under the scaling $\nu_n/n \rightarrow 0$, the entries of $(\rho_{k\ell})$ do not. To guarantee that $\omega_2 > 0$, it is enough that the $K_0 \times K_0$ matrix $(B_{k\ell}^0 \widetilde{\pi}_\ell)$ has no two colinear rows, a mild identifiability condition.

The above argument also shows the advantage of using $K+1$ communities when compressing the columns: In testing the null hypothesis $K = K_0 - 1$, the multinomial parameters ρ_{k*} match (roughly) their true versions based on B^0 and θ (ignoring the randomness in S_1). This increases the power of the test, since at least two row communities that are merged together (due to fitting $K_0 - 1$ communities to the rows) will have ρ parameters based on distinct rows of B^0 . When underfitting with $K \leq K_0 - 2$, the column communities are mixed ($L < K_0$), hence the rows of ρ will be a (scaled) weighted mixture of the rows of B^0 . These mixtures still lead to an ω_2 that is bounded away from zero, provided that the mixture weights do not converge to specific values that make the rows of ρ identical, a highly implausible situation. One can say more if the community detection algorithm is known to recover a superset of the true communities when underfitting, as shown, for example, for the spectral clustering in [MSZ18]. We, however, note that recovering a superset is not required for SNAC+ to be consistent. We refer to [WB17] for an example of how the weighted mixture of the rows of the connectivity matrix B emerges in the underfitted case.

4.2 Comparison with the existing literature

The closest work in the literature to ours is the spectral goodness-of-fit test for SBMs [BS16; Lei16]. Roughly speaking, Lei [Lei16] shows that, under a K -SBM, $n^{2/3}(\sigma_1(\tilde{A}) - 2)$ has a type-1 Tracy-Widom distribution asymptotically, where $\sigma_1(\cdot)$ denotes the largest singular value, and \tilde{A} is a standardized version of the adjacency matrix, calculated based on fitting a K -SBM (see Section 5.1). This result requires the entries of the connectivity matrix B to be bounded away from zero which excludes the sparse regime $\nu_n/n \rightarrow 0$ we consider here. Moreover, Lei's Theorem 3.3 provides an asymptotic power guarantee. Translating the results to our notation, assuming that the true model has more communities than the fitted model, the result shows that $n^{2/3}\sigma_1(\tilde{A}) \gtrsim \nu_n n^{1/6}$ w.h.p. Since under the true model $n^{2/3}\sigma_1(\tilde{A}) \approx 2n^{2/3}$,

one obtains a consistent test as long as $\nu_n n^{1/6} \gg n^{2/3}$, that is, $\nu_n \gg n^{1/2}$. This required scaling is in fact better than what is stated in [Lei16]. Nevertheless, $\nu_n \gg n^{1/2}$ is far from the sparse regime $\nu_n \asymp \log n$ that our results allow. More importantly, it is not clear how to extend the spectral test to the degree-corrected setting. In Section 5.1, we discuss the natural extension of the spectral test to the DCSBM and study its performance empirically. Due to the difficulty of estimating the θ parameter of DCSBM, theoretical guarantees for this (naive) extension are not easy to obtain. Our SNAC+ test avoids explicitly estimating θ , by conditioning on the degrees which leads to the cancellation of individual θ_i in the resulting multinomial distributions. In practice, convergence to the Tracy-Widom distributions is known to be slow, whereas convergence to the normal distribution for SNAC+ happens quite fast (at a rate at most $\approx \nu_n^{-1/2}$ as we showed).

Another work with connections to ours is that of Karwa et al. [Kar+16] where chi-square statistics for the goodness-of-fit testing of SBM and β -SBM are proposed. They introduce a block-corrected chi-square statistic for the SBM that uses the idea of block compression and has resemblance to our NAC statistics. The similarity is, however, superficial, since we work conditional on the degrees, hence the parameters we consider are not the connectivity parameters B but their normalized versions ρ (compare equation (5) in [Kar+16] with our equation (17)). The ρ parameters have many desirable features; for example, they do not vanish in the sparse regime ($\nu_n/n \rightarrow 0$) while the connectivity parameters B do, making the corresponding chi-square statistic numerically very unstable (due to the division by these vanishing parameters). The cancellation of the degree-propensity parameters θ_i in ρ is another key advantage, allowing us to use the same statistic in the degree-corrected case. In contrast, Karwa et al. [Kar+16] devise another test (with no compression) for the β -SBM (a close cousin of DCSBM, in the sparse regime) which requires $O(n^2)$ operations to compute. Another novelty of our approach relative to [Kar+16] is the idea of block compression with $K + 1$ communities instead of K which leads to a dramatic increase in the power of the test.

Another major difference with [Kar+16] is their interest in computing exact p -values which requires enumerating all graphs with a given sufficient statistic as the observed one. (For example, for an SBM with known community structure, this translates to enumerating all graphs that have the exact same number of edges between communities as that of the observed network). Although, Karwa et al. develop clever sampling schemes to traverse this space, to get an accurate p -value, one has to sample a prohibitively large number of graphs in general, rendering the approach infeasible beyond small networks. In addition, their main arguments are for block models with a given community structure, and to get around the unknown nature of the communities in practice, they propose sampling the community labels and applying the known-community test on each. The space of all labels is again exponentially large (of size K^n), and one requires a very large sample to get any reasonable estimate, making the approach infeasible for large networks. The authors acknowledge this difficulty and suggest using labels obtained by spectral clustering in practice. One then has to worry about the dependence of these labels on the same data the test is computed from, a point where we carefully address in this paper. The asymptotic distributions we obtain for the adjusted statistics are very good approximations for large networks and allow us to apply the tests with minimal computational overhead to even networks of millions of nodes.

Compared with likelihood ratio (LR) tests [Yan+14b; WB17], our approach is more general since LR tests require a specific alternative model to compare with (often another SBM or

DCSBM), while in goodness-of-fit testing, only the null has to be specified. In addition, rigorous results on LR tests, such as [WB17], often work with a computationally intractable version of the test where the label parameter z is marginalized by summing over K^n possibilities. In practice, these tests are often implemented by approximating the sum via variational inference for which the theoretical guarantees do not extend. We discuss another approximate implementation in Section 5.1 and compare with it in simulations.

A pseudo-LR approach with rigorous guarantees is developed in [MSZ18]. As in [WB17], the focus there, too, is on model selection and comparing DCSBM models, specifying both the null and alternative models, in contrast to NAC tests. Our approach is comparable to that of [MSZ18] when applied sequentially for model selection, but NAC family of tests are computationally more efficient: (1) Computing the test statistic of [MSZ18] has $O(n^2)$ computational complexity, whereas due to the column compression, we require only $O(M)$ where M is the number of edges. (2) [MSZ18] creates new labels by binary segmentation, but we save time by reusing the labels estimated by the community detection algorithm. In addition, their consistency results are based on the assumption that the community detection algorithm merges the true communities when it underfits and splits them when it overfits. However, our test only imposes the mild assumption that connectivity parameters are distinguishable among communities, allowing it to be compatible with many community detection algorithms.

As for the degree requirement, our method only requires $\nu_n \gtrsim \log n$, similar to model selection approaches in [MSZ18; LL15; CL18], and slightly better than those of [LLZ20; WB17] that require $\nu_n / \log n \rightarrow \infty$. In contrast, the spectral goodness-of-fit test [BS16; Lei16] has a much more severe requirement ($\nu_n \gg n^{1/2}$) as discussed earlier.

5 Numerical Experiments

We now illustrate the performance of NAC+ and SNAC+ on simulated and real networks. We use regularized spectral clustering [Ami+13] as the community detection algorithm, since it is widely used, computationally efficient and conjectured to satisfy Assumption 1 [Abb+20]. Given the number of communities K , the spectral clustering estimates the community labels by applying k -means clustering to the rows of the matrix formed by the K leading eigenvectors of the normalized Laplacian. Regularization is attained by adding $\tau d_{\text{av}}/n$ (where d_{av} is the network average degree) to every entry of the adjacency matrix before forming the Laplacian. This regularization is known to improve the performance in the sparse regime ($d_{\text{av}} \ll n$) [LLV17; ZR18].

5.1 Other methods

Along with the NAC tests, we consider the following approaches for comparison: Likelihood ratio test (LR) [WB17], Bayesian information criteria (BIC) [WB17], adjusted spectral test (AS) [Lei16], Bethe-Hessian spectral approach (BH) [LL15], network cross-validation (NCV) [CL18] and edge cross-validation (ECV) [LLZ20]. In each case, we add the suffix “boot” to the name, if bootstrap debiasing of Section 3.3 is applied to further adjust the statistic. Our implementation of LR, BIC and AS is slightly different from the corresponding references, as discussed below.

Let $\ell(B, \theta, \pi, z | A) = \sum_i \log \pi_{z_i} + \sum_{i < j} \phi(A_{ij}; \theta_i \theta_j B_{z_i z_j})$ be the log-likelihood of a DCSBM where π is the class prior. We consider a Poisson likelihood rather than a Bernoulli one, mainly

due to its computational efficiency for large sparse networks, hence $\phi(x; \lambda) = x \log \lambda - \lambda$. In contrast to [WB17] who sum over z (and marginalize θ too, by putting a Dirichlet prior on it), we compute $\ell(\hat{B}, \hat{\theta}, \hat{\pi}, \hat{z} | A)$ where \hat{z} is the label estimate from the spectral clustering and \hat{B} , $\hat{\theta}$ and $\hat{\pi}$ are the natural estimates based on \hat{z} , that is,

$$\hat{B}_{k\ell} = \frac{N_{k\ell}(\hat{z})}{m_{k\ell}(\hat{z})}, \quad \hat{\theta}_i = \frac{n_{\hat{z}_i}(\hat{z})d_i}{\sum_{j:\hat{z}_j=\hat{z}_i} d_i}, \quad \hat{\pi}_k = n_k(\hat{z})/n$$

where $N_{k\ell}(\hat{z})$ is the sum of the elements of A in block (k, ℓ) specified by labels \hat{z} , $n_k(\hat{z})$ is the number of nodes in community k according to \hat{z} and $m_{k\ell}(\hat{z}) = n_k(\hat{z})(n_\ell(\hat{z}) - 1\{k = \ell\})$. We note that \hat{B} is the same as the natural estimate of B in the SBM.

The LR test computes $\ell(\hat{B}, \hat{\theta}, \hat{\pi}, \hat{z} | A)$ for two DCSBMs with different number of communities and compares the difference to a threshold. The BIC score is $\ell(\hat{B}, \hat{\theta}, \hat{\pi}, \hat{z} | A) - K(K + 1) \log n/2$ which is maximized to select the optimal K . For the AS, we consider the adjusted matrix $\tilde{A} = (\tilde{A}_{ij})$ where

$$\tilde{A}_{ij} = (A_{ij} - \hat{P}_{ij})/(n\hat{P}_{ij})^{1/2}, \quad \hat{P}_{ij} = \hat{\theta}_i \hat{\theta}_j \hat{B}_{\hat{z}_i, \hat{z}_j} \cdot 1\{i \neq j\} \quad (26)$$

and compute its largest singular value $\sigma_1(\tilde{A})$. The difference with [Lei16] is that we are using the (estimated) Poisson variance \hat{P}_{ij} rather than the Bernoulli variance $\hat{P}_{ij}(1 - \hat{P}_{ij})$. Moreover, we use the DCSBM estimate of mean matrix (P_{ij}) . Using the Poisson variance significantly improves the computational performance for sparse matrices, since then \tilde{A} can be written as the sum of a sparse matrix and a term involving the product of diagonal and low-rank matrices. This allows fast computation of $\tilde{A}x$ for any vector x , hence allows the singular value computation to scale to very large networks.

In some simulations, we also consider AS-SBM, where we use the SBM estimate for \hat{P}_{ij} , which is obtained by setting $\hat{\theta}_i = 1$ in (26). Using the same arguments as in [Lei16], one can show that in the case of AS (SBM), under a Poisson-SBM null, the distribution of $\sigma_1(\tilde{A})$ will be close to the Tracy-Widom distribution with index 1. However, the same cannot be said about AS which uses the DCSBM estimate of (P_{ij}) . Nevertheless AS is the natural version to consider when fitting DCSBMs.

5.2 Simulations

As discussed earlier, a goodness-of-fit test can be used in a sequential manner to perform model selection. We now provide simulations showing that, when applied sequentially, the family of NAC+ are consistent, and competitive with other model selection approaches. Here, we report results for samples from Bernoulli DCSBMs. Since we work with sparse networks, the Bernoulli model will be very close to its Poisson version. This was empirically confirmed, as we did not see a significant drop in performance for the NAC+ tests in our simulations, under a Bernoulli model relative to the Poisson.

5.2.1 Model selection performance

Let $\text{Pareto}(x_0, \alpha)$ denote a Pareto distribution with scale parameter x_0 and shape parameter α , so that its mean is $\alpha x_0 / (\alpha - 1)$. We simulate data from a K -block DCSBM with connection propensity $\theta_i \sim \text{Pareto}(3/4, 4)$, and a connectivity matrix which is one of the following:

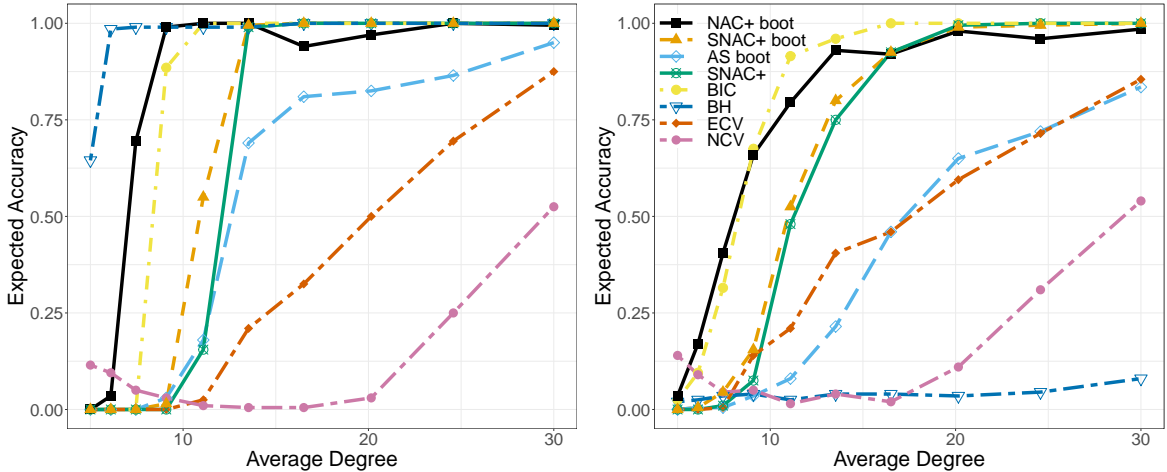


Figure 1: Expected accuracy of selecting the true number of communities versus expected average degree of the network. The data follows a DCSDM with $n = 5000$, $K = 4$, $\theta_i \sim \text{Pareto}(3/4, 4)$ and balanced community sizes. The connectivity matrices are B_1 (left) and B_2 (right), as defined in the text.

1. $B_1 \propto (1 - \beta)I_K + \beta \mathbf{1}\mathbf{1}^T$, that is, a simple planted partition model with out-in-ratio β ,
2. $B_2 \propto \gamma R + (1 - \gamma)Q$, where $\gamma \in (0, 1)$, R is a random symmetric permutation matrix, and Q a symmetric matrix with i.i.d. $\text{Unif}(0, 1)$ entries on and above diagonal.

Here, $\mathbf{1}$ is the all-ones vector. In both cases, the matrices are normalized to have a given expected average degree λ . The simple planted partition model B_1 generates a very homogeneous assortative network. Model B_2 creates a more general model by employing the permutation, allowing a mix of assortative and disassortative communities. Model B_2 is in general harder to fit.

Figure 1 illustrates the model selection accuracy of various methods for the following setup: $n = 5000$, true $K = 4$ with balanced community sizes, $\beta = 0.2$ and $\gamma = 0.3$. For the goodness-of-fit tests NAC+, SNAC+ and AS, we use sequential testing from below to estimate K . In each case, the rejection threshold is set to have a significance level of 10^{-6} (under null). For tests with bootstrap debiasing, the number of bootstrap simulations is 10. Figure 1 shows the expected model selection accuracy versus the expected average degree λ for each method. The accuracy is obtained by averaging over 200 replications. As λ increases, the problem gets easier and we expect the performance of consistent methods to improve.

For both models B_1 and B_2 , the performance of NAC+ and BIC are close and they outperform other approaches, except for the BH in the case of the B_1 model. Note, however, that BH performs extremely poorly under B_2 , showing that associativity is necessary for its consistency. In fact, as pointed out in [LL15], BH requires all the eigenvalues of $\mathbb{E}[A]$ to be positive, which is violated with positive probability under the B_2 model. The two versions of SNAC+ perform very close to each other and ranked after the NAC+ and BIC pair. That the performance of the bootstrap SNAC+ is very close to that of SNAC+ with the theoretical threshold, corroborates the accuracy of the null distribution in Theorem 2. The spectral test (AS) performs reasonably well for model B_1 , albeit ranked after SNAC+, but relatively poorly under B_2 . The cross-validation approaches generally underperform other approaches for model

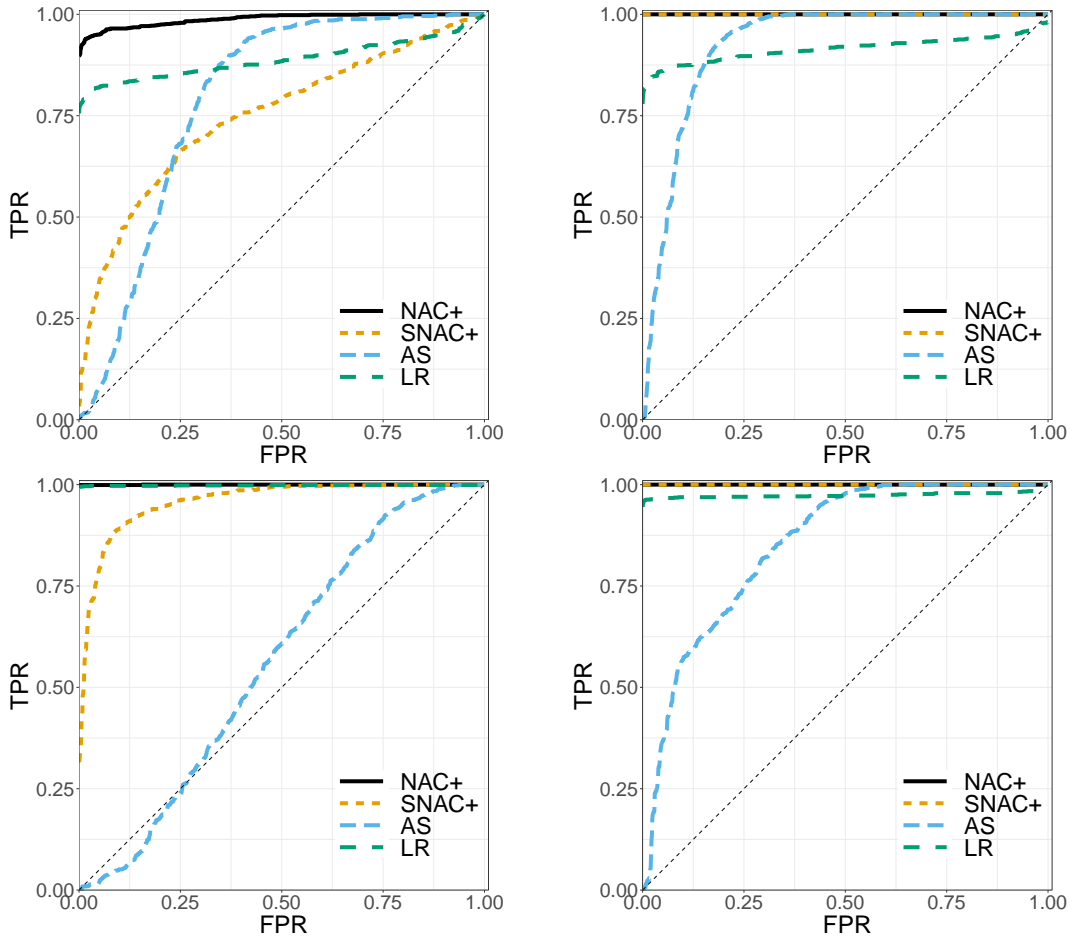


Figure 2: ROC plots for testing 4 versus 5 community models. Top and bottom rows correspond to $n = 2000$ and $n = 10000$, respectively. Left and right columns correspond to the DCSBM and DCLVM alternatives, respectively.

selection, with ECV significantly outperforming NCV.

It is also possible to construct examples where NAC+ significantly outperforms BIC. See Figure 8 in the Supplement for one such case.

5.2.2 ROC curves

Another way to measure the performance of a test statistic is by means of its Receiver Operating Characteristic (ROC) curve, that is, the power of the test as a function of Type I error; equivalently, the true positive rate (TPR) as a function of the false positive rate (FPR). The ROC curve reveals the best possible performance of a statistic for a given testing problem (one achieved by setting the optimal threshold). Here, we compare the ROC curves of the NAC+ tests to the likelihood ratio (LR) and spectral (AS) test, for the problem of testing the null hypothesis of $K = 4$ versus the alternative of $K + 1 = 5$ communities. This is an example of “testing from below” which is encountered in sequential model selection.

For the null hypothesis, we consider a simple DCSBM with $K = 4$ communities, having a

connectivity matrix of type B_1 , introduced in Section 5.2.1, with $\beta = 0.1$. For the alternative, we consider two cases: (a) a DCSBM with $K + 1 = 5$ and otherwise similar parameters to the null DCSBM, and (b) a degree-corrected latent variable model (DCLVM) with $K + 1 = 5$ communities generated as follows: Given a set of latent node variables $\{x_i\}_{i=1}^n \subset \mathbb{R}^d$ with $d = K + 1$, the adjacency matrix $A = (A_{ij})$ is generated as a symmetric matrix, with independent Bernoulli entries above the diagonal, with

$$\mathbb{E}[A_{ij} | x, \theta] \propto \theta_i \theta_j e^{-\|x_i - x_j\|^2} \quad \text{and} \quad x_i = 2e_{z_i} + w_i \quad (27)$$

where e_k is the k th basis vector of \mathbb{R}^d , $w_i \sim N(0, I_d)$ and $\{z_i\} \subset [K + 1]^n$ are multinomial labels (similar to the DCSBM labels). In other words, the latent positions $\{x_i\}$ are drawn from a Gaussian mixture model with $K + 1 = 5$ components, living in \mathbb{R}^{K+1} . The proportionality constant in (27) is chosen such that the overall network has expected average degree λ . For all the models, including the null and the two alternatives, the underlying prior on the labels is taken to be proportional to an arithmetic progression: $\mathbb{P}(z_i = k) \propto k$ to produce unequal community sizes, and we let $\theta_i \sim \text{Pareto}(3/4, 4)$ and $\lambda = 15$.

Figure 2 illustrates the resulting ROC curves. As expected, increasing n generally improves the performance (except for AS). Both NAC+ and LR are almost perfect tests for differentiating the two DCSBMs at $n = 10^4$. In all cases, the NAC+ is more powerful than the sub-sampled version, SNAC+. This is expected since SNAC+ relies on half the data. Note that as n increases, SNAC+ greatly improves which can be attributed to the label estimation procedure achieving almost exact recovery, even at half the size of the original network. Note that AS generally is much less competitive compared to LR or NAC+. This is expected since the spectral test relies on a general statistic that is not tailored to the blocked nature of the adjacency matrix of a DCSBM.

Interestingly, both NAC+ and SNAC+ are almost perfect tests for DCLVM even at $n = 2000$, whereas LR test underperforms under the DCLVM. This is also expected, since the LR test incorporates the likelihood of a DCSBM for the alternative, which is mismatched to the actual alternative model. This experiment shows the power of NAC+ family in rejecting against models outside the family of DCSBM. It highlights the advantage of goodness-of-fit over likelihood-ratio testing where one does not have to specify explicitly alternatives, hence can test against many alternatives simultaneously. Companion results for the problem of testing 4 versus 3 communities are reported in Figure 9 in the Supplement.

5.3 Goodness-of-fit testing

The main utility of a goodness-of-fit test is to assess how well real data fits the model. Let us investigate how well a DCSBM fits the real networks from the Facebook-100 dataset [Tra+11; TMP12], hereafter referred to as FB-100. This dataset is a collection of 100 social networks, each the entire Facebook network within one university from a date in 2005. The networks vary considerably in size and degree characteristics; some statistics are provided in Table 1.

Figure 3 shows the violin plots of the SNAC+ statistic versus the number of communities for the entire FB-100 data. The variation at each K is due to the variability of SNAC+ over the 100 networks in the dataset. For comparison, the violin plots are also shown when SNAC+ is applied to a sample of size 100 from a DCSBM model with $K = 3$ communities. In this case, the 100 simulated networks are generated with the number of nodes and average

	Min.	1st Qu.	Median	Mean	3rd Qu.	Max.
n	769	4444	9950	12083	17033	41554
Mean deg.	39	65	77	77	88	116
3rd Qu. deg.	54	91	110	108	124	166
Max. deg.	248	673	1202	1787	2123	8246

Table 1: Statistics on the FB-100 dataset. Qu. is a short-hand for quartile.

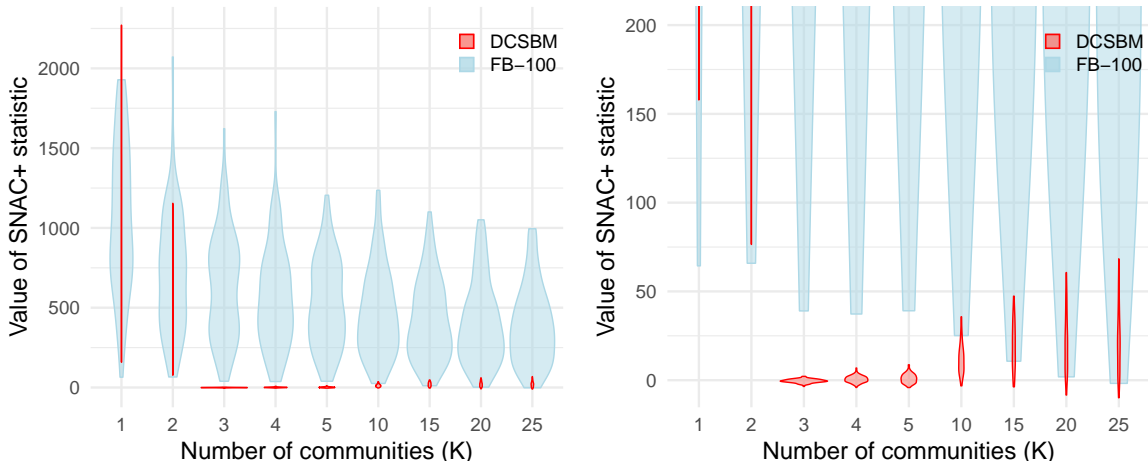


Figure 3: Comparing the goodness-of-fit of DCSBM to the FB-100 dataset versus a dataset simulated from a DCSBM with $K = 3$ communities, having the same size and average degree characteristics as that of FB-100. The left plot is the zoomed-in version of the right plot.

degrees matching those of the FB-100 network. The DCSBM is otherwise a simple one with connectivity matrix B_1 , out-in-ratio = 0.1 and propensity parameter $\theta_i \sim \text{Pareto}(3/4, 4)$. The plots show a marked deviation of FB-100 networks from a DCSBM model as measured by SNAC+ goodness-of-fit test. If the networks were generated from a DCSBM, one would expect the distribution of SNAC+ to drop to within a narrow band around zero once K surpasses the true number of communities. Only at $K = 25$ a small fraction of FB-100 networks have SNAC+ values within, say, the interval $[-5, 5]$, showing that a DCSBM with $K < 25$ is not a good model for any of these networks. Even at $K = 25$, the majority of FB-100 networks are still ill-fitted.

On the other hand, we observe that for the simulated data, SNAC+ drops to a narrow band around zero for $K = 3$, while remaining large for $K = 1$ and $K = 2$. This corroborates the results of both Theorem 1 and Theorem 3 that predict exactly this behavior. Note that this conclusion holds despite the variation in the sizes and average degrees of the simulated networks, showing the insensitivity of the null distribution of SNAC+ to those parameters, as predicted by the theory.

Examining the FB-100 data further, one observes that most networks show some very high degree nodes that seem to skew the result of community detection as well as graph drawing algorithms. This can also be inferred from the significant divide between the third quartile and the maximum degree in Table 1. Le, Levina, and Vershynin [LLV17] have also shown that abnormally high degrees can obstruct community detection. Treating these high-degree nodes

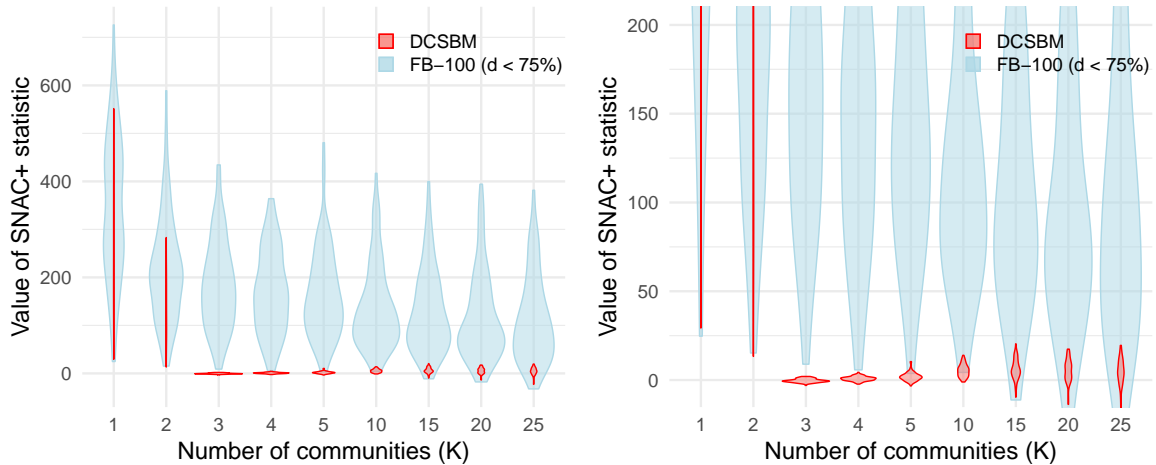


Figure 4: Similar to Figure 3 but with Facebook networks reduced by restricting to nodes with degrees below the 75 percentile.

as outliers, one could ask what happens if we remove them and refit the model? Figure 4 shows the result of performing the same experiment, but applied to the *reduced* FB-100 networks, obtained by restricting to the (induced) subnetwork formed by nodes having degrees below the 3rd quartile (i.e., the 75 percentile). Table 2 shows the statistics on these reduced networks, revealing less skewed degree distributions compared to the original data. Figure 4 shows that the reduction leads to an overall improvement in the fit: More networks have SNAC+ values that drop to near zero and this happens for lower values of K . This shows the effectiveness of goodness-of-fit testing, in the sense that it allows us to test the hypothesis that removing the high-degree nodes causes a better DCSBM fit. Nevertheless, Figure 4 shows that the majority of the reduced networks are still far from a DCSBM with few number of communities.

	Min.	1st Qu.	Median	Mean	3rd Qu.	Max.
n	544	3293	7356	8930	12601	30590
Mean deg.	11	20	24	24	28	36
3rd Qu. deg.	16	29	34	34	40	52
Max. deg.	38	74	89	87	101	149

Table 2: Statistics on the reduced FB-100 dataset.

5.4 Exploring community structure

As demonstrated in Section 5.3, a DCSBM (with small K) is not a good fit for most of the networks in FB-100. Even in such cases, SNAC+ has utility beyond testing and can be used to reveal community structure in networks. We demonstrate this by using the reduced FB-100 networks constructed in Section 5.3. Recall that SNAC+ quantifies the similarity within each estimated community, and a smaller value means that the rows in an estimated community share a similar connection pattern to other communities. Therefore, sharp drops in the value of SNAC+, as K varies can signal the existence of community structure. For a sequence of

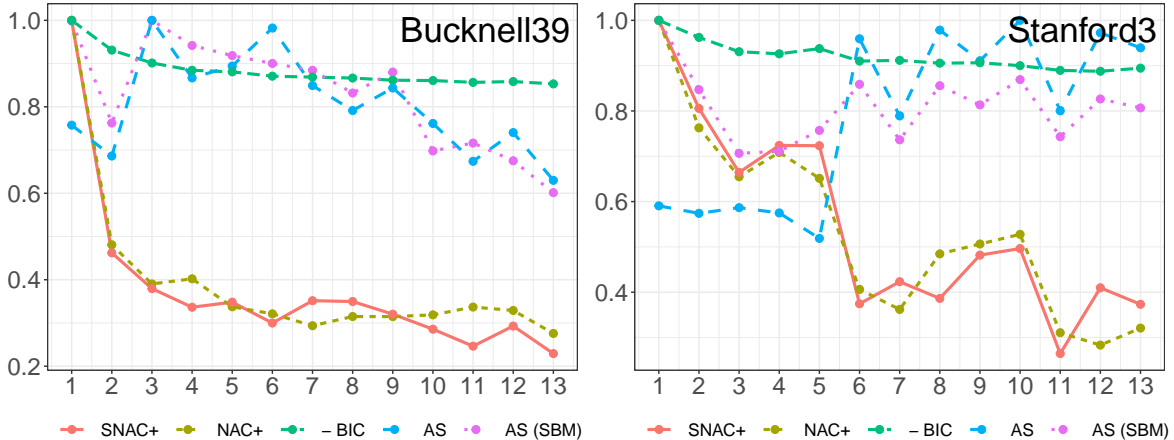


Figure 5: Normalized statistics versus the candidate number of communities (K).

SNAC+ statistics with increasing K , there could be an *elbow* where continuing to increase K does not bring a significant decrease in the statistic, or a *dip* where SNAC+ starts to increase. These two types of points signal that it is not worthwhile to continue increasing K . Furthermore, these transitions are often much more dramatic for NAC+ family of tests than the competing methods and can be easily identified by eyeballing the plots.

Figure 5 shows the normalized statistic plots for two networks from FB-100. The plots show the normalized value of SNAC+, NAC+, AS, AS-SBM and negative BIC statistics for $K = 1, \dots, 13$. The statistics are normalized to fall in the range $[-1, 1]$ by dividing by their largest absolute value, for each test, respectively. This allows us to compare the trend of each statistic as K increases among different methods.

For many of the FB-100 networks, SNAC+ and NAC+ share a similar pattern, with rapid drops followed by the flattening or increase of the statistic, signaling strong community structures. In contrast, AS and AS-SBM generally do not show strong trends, while negative BIC barely fluctuates at all when K increases. For example, for the Bucknell network (Figure 5), there is one sharp elbow at $K = 2$ for the NAC+ tests. The Stanford network shows an elbow/dip at $K = 3$ and a similar elbow/dip at $K = 6$ in NAC+ tests. This suggests that the network has two levels of community structure (cf. Figure 7), an interesting phenomenon not captured by other statistics. Note that AS-SBM captures the community structure at $K = 3$ for the Stanford network (with a dip at $K = 3$) while missing the $K = 6$ possibility. The AS version (employing degree-correction) behaves contrary to expectation in this case and misses both structures.

Community profiles. We now consider a more quantitative approach to constructing a community profile based on the value of SNAC+. We take advantage of the randomness in SNAC+ due to subsampling, as a natural measure of the uncertainty of the community structure. For each K , we calculate SNAC+ several times (each time using a random split of the nodes) and then fit a smooth function to the resulting points, treating the problem as a nonparametric regression. Here, we consider smoothing splines but other approaches such as Gaussian kernel ridge regression can be equally useful. The estimated smooth function

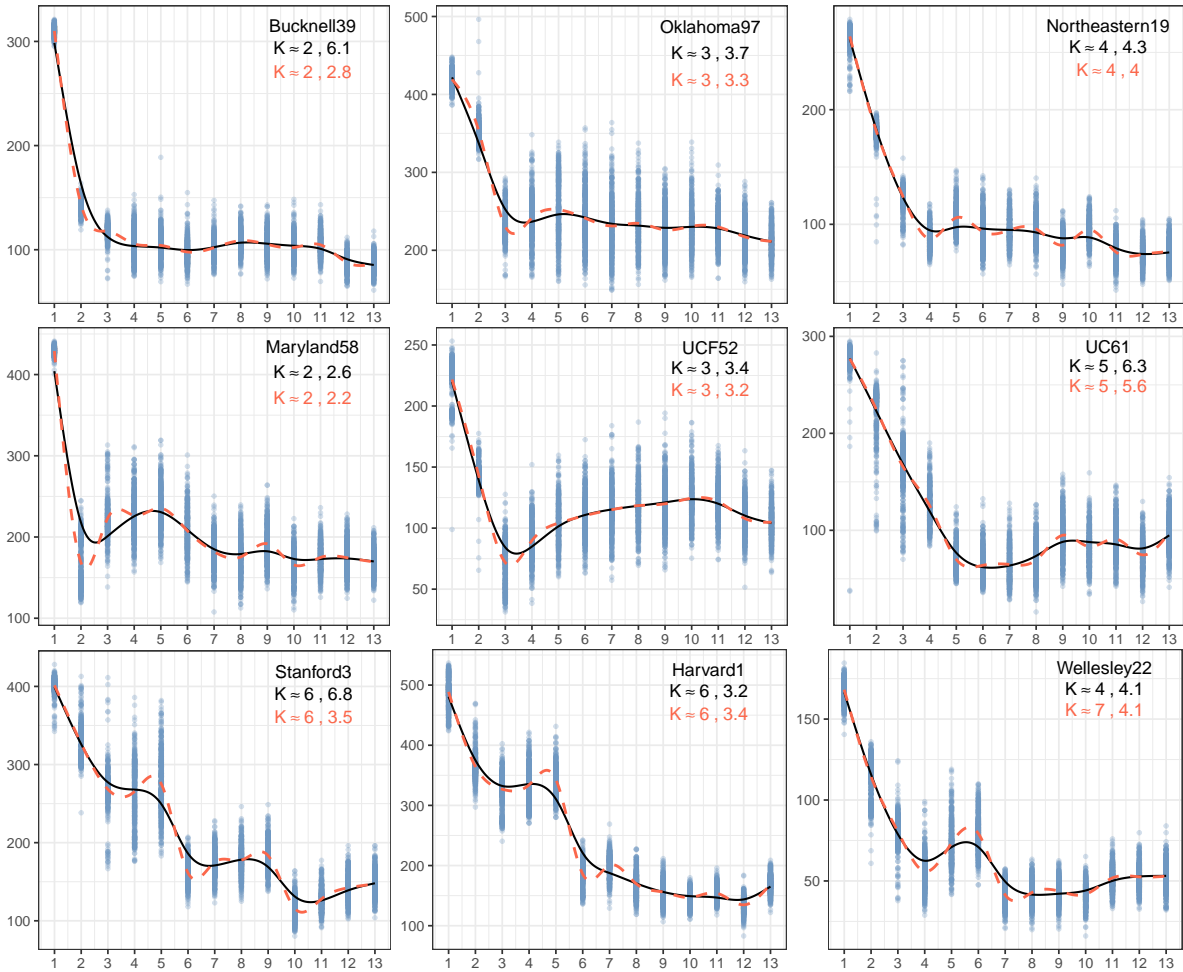


Figure 6: Community profile plots. The solid and dashed lines show the smoothed SNAC+ statistic versus the candidate number of communities (K). The dots each represent the SNAC+ value for a random split of the network. The difference between the solid and dashed lines is the smoothness level of the fitted smoothing spline.

provides what we refer to as *a community profile* for the network. This profile can be used for comparing and classifying networks as well as determining possible good choices of the number of communities. The subsampling and smoothing provide a degree of robustness to these profiles as illustrated below.

Instead of eyeballing a plot for its elbows and dips, we can rely on the derivatives of the community profile to guide us. We quantify the elbow as the point where the second derivative has the largest value and the dip as where the first derivative turns positive for the first time. Alternatively, one can use the the point with the largest curvature as the elbow point [HO93]. However, we have found, empirically, that the second derivative, as a proxy for the curvature, is much more accurate in capturing the elbow as determined by a human observer.

Figure 6 provides instances of three most common patterns of community profiles for the FB-100 networks. For each plot, we show community profiles using two smoothness levels: (1) the dashed red line corresponding to smoothness level set by generalized cross-validation

(GCV) [GHW79], and (2) the solid line providing a smoother fit, corresponding to `spar` = 0.3, where `spar` is the smoothness parameter in base R’s implementation of smoothing splines. The GCV version is usually rougher and captures subtle changes, whereas the solid black fit is smoother and more robust. For each of the two fitted curves, the values of K corresponding to the elbow and dip, as estimated by the derivatives, are given on each plot (with the elbow point recorded first). For example, the Harvard network shows an elbow at $K = 6$ and a dip at $K \approx 3.2$ according to the smoother profile. Compared with normalized plots (Figure 5), community profiles show less randomness and the quantified elbows and dips are consistent with those identified by a human observer. It is worth noting that our maximum second derivative criterion for identifying the elbows, surprisingly, almost always returned an integer in these experiments (i.e., no rounding is performed in reporting the elbow points).

The first row in Figure 6 shows a single-elbow pattern, and the second row a single first dip (possibly followed by minor smaller dips later on). The third row illustrates a pattern with more than one significant drop, corresponding to multiple elbow/dips. This interesting multi-stage behavior is exhibited by a few of the FB-100 networks, and suggests the possibility of breaking the networks into communities in multiple (potentially hierarchical) ways. As mentioned earlier, these multi-stage structures are only captured by SNAC+ among the competing methods. This case illustrates the subtlety of community detection in real networks, showing that insisting on fitting the networks with a single K could lead to missing interesting substructures. We also point out that having an elbow/dip at $K = 2$ is very common for the FB-100 networks; we refer to the additional profile plots provided in the Supplement.

Note that in addition to revealing community structure, the absolute value of the profile curves in Figure 6 is also informative and measures the distance of the network from a DCSBM. Since SNAC+ is guaranteed to be centered around zero under a DCSBM, the networks with a larger absolute value of SNAC+ are further away from a DCSBM. For example, Figure 6 shows that Wellesley with $K = 4$ communities, having an average SNAC+ value ≈ 60 is a much better fit to DCSBM than Maryland with $K = 2$ communities, showing an average SNAC+ value ≈ 200 .

Figure 7 shows community structure of some of the FB-100 networks with nodes colored according to their estimated community label. The Stanford and Harvard networks are shown both with $K = 3$ and $K = 6$ estimated communities, as suggested by the two stages of their community profiles. We note that for both of these networks either of these two divisions into communities is visually sensible, with $K = 6$ apparently capturing more refined substructures within the $K = 3$ division. (It is interesting to note that the $K = 6$ partition in each case is not a strict refinement of the $K = 3$ partition, but rather close to being a refinement.) The community structures shown for Maryland and Northeastern are based on the optimal K predicted by their profile plots, and they too make sense visually.

In the Supplement, we also provide normalized and profile plots (Figure 13) for the political blog network [AG05] which is widely used as a benchmark for community detection. The profile plot shows an elbow at $K = 2$, as identified by the second derivative, matching the expected ground truth of two communities corresponding to the Democratic and Republican parties.

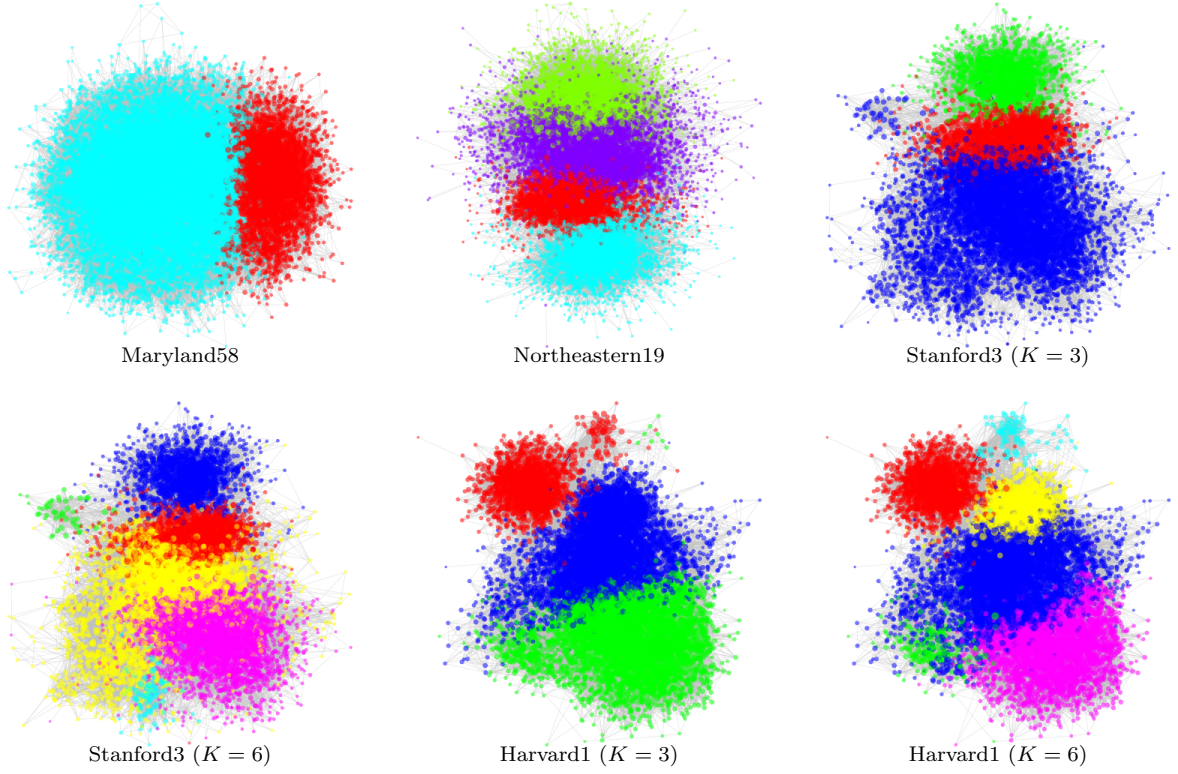


Figure 7: FB-100 network plots. The colors specify the estimated communities.

6 Proofs

In this section, we prove Theorems 2 and 3. The proof of Theorem 1 is deferred to the Supplement. We start by setting up notation and deriving some preliminary results that are common to both proofs. We often work conditioned on S_1 , $A_{S_1 S_1}$ and $(d_i, i \in S_2)$. Let \mathcal{F} be the σ -field generated by these variables:

$$\mathcal{F} = \sigma(S_1, A_{S_1 S_1}, (d_i, i \in S_2)), \quad (28)$$

and let $\mathbb{E}^{\mathcal{F}}$ and $\mathbb{P}^{\mathcal{F}}$ denote the expectation and probability operators, conditioned on \mathcal{F} . We assume without loss of generality that the community detection algorithm is nonrandomized, so that conditioned on \mathcal{F} , \hat{y} is fixed. (Otherwise, we add the independent source of randomness used by the algorithm to \mathcal{F} .) Throughout, K_0 denotes the true number of communities.

Recall that $S_1 \subset [n]$ is determined by including any element of $[n]$ with probability $1/2$, and $S_2 = [n] \setminus S_1$. Then, $d_i := \sum_{j \in S_1} A_{ij} = \sum_{j=1}^n A_{ij} U_j$ where $U_j = 1\{j \in S_1\}$, $j \in [n]$ is an independent $\text{Ber}(1/2)$ sequence. Letting $d_i^* = \mathbb{E}[d_i]$, we have

$$d_i^* = \frac{1}{2} \sum_{j=1}^n \mathbb{E}[A_{ij}] = \frac{1}{2} \theta_i a_{z_i}, \quad \text{where} \quad a_h := \sum_{k=1}^{K_0} B_{hk} \sum_{j \in \mathcal{C}_k} \theta_j \quad (29)$$

for all $h \in [K_0]$. Here, $\mathcal{C}_k = \{i \in [n] : z_i = k\}$ is the true community k , and we let $n_k = |\mathcal{C}_k|$.

We also let $\mathcal{G}_k := \{i \in S_2 : z_i = k\} = \mathcal{C}_k \cap S_2$. We often work on the following event:

$$\mathcal{A} = \left\{ |\mathcal{G}_k| \in [0.4n_k, 0.6n_k], \forall k \in [K_0] \right\} \cap \left\{ d_i \in \left[\frac{d_i^*}{2}, \frac{3d_i^*}{2} \right], \forall i \in [n] \right\}. \quad (30)$$

Note that \mathcal{A} is deterministic conditioned on \mathcal{F} . The next lemma guarantees that this event holds with high probability:

Lemma 1. *Under the scaling assumption (23), $\mathbb{P}(\mathcal{A}^c) \leq 7n^{-1}$.*

Let us derive some bounds on d_i^* . Recalling that $\theta_{\max} = 1$,

$$a_h \geq \tau\theta_{\max}n_k \sum_k B_{hk} = \tau\theta n_k \frac{\nu_n}{n} \|B_{h*}^0\|_1 \geq \tau\theta\nu_n\tau_C \min_{h'} \|B_{h'*}^0\|_1. \quad (31)$$

Using the definition of C_1 in (21), we obtain

$$d_i^* \geq \frac{1}{2}C_1\nu_n, \quad \forall i. \quad (32)$$

Let $a_{\max} = \max_h a_h$. Since $|\mathcal{C}_k| \leq n$, we have $a_{\max} \leq \nu_n \cdot \max_h \|B_{h*}^0\|_1$. Combining with assumption (31), we obtain

$$a_h \geq \tau_a a_{\max}, \quad \tau_a := \tau\theta\tau_B\tau_C. \quad (33)$$

Since $\|B^0\|_\infty = 1$ by assumption, we have

$$d_i^* \leq \frac{1}{2}K_0\nu_n, \quad \forall i. \quad (34)$$

By the stability assumption 1, for all $k \in [K_0]$ and $\ell \in [L]$,

$$\rho_{k\ell} = \frac{\sum_{h=1}^{K_0} B_{kh}^0 R_{h\ell}}{\sum_{\ell'=1}^L \sum_{h=1}^{K_0} B_{kh}^0 R_{h\ell'}} \geq \tau_B\tau_\theta \frac{\sum_{j \in S_1} 1\{\hat{y}_j = \ell\}}{|S_1|} \geq \tau_B\tau_\theta\tau_0 = \tau_\rho. \quad (35)$$

It follows that $\rho := \min_{k,\ell} \rho_{k\ell} \geq \tau_\rho$.

6.1 Proof of Theorem 2

For a random variable Y , let $\mathcal{L}(Y | \mathcal{F})$ be the law of Y conditioned on \mathcal{F} and let

$$d_K(\mathcal{L}(Y | \mathcal{F}), Z) = \sup_{t \in \mathbb{R}} |\mathbb{P}(Y \leq t | \mathcal{F}) - \mathbb{P}(Z \leq t)|. \quad (36)$$

Lemma 2. *For any random variables, Y and Z , any event \mathcal{B} and any σ -field \mathcal{F} , we have*

$$\begin{aligned} d_K(Y, Z) &\leq \mathbb{E}[d_K(\mathcal{L}(Y | \mathcal{F}), Z)], \\ |d_K(Y, Z) - d_K(Y1_{\mathcal{B}}, Z)| &\leq \mathbb{P}(\mathcal{B}^c). \end{aligned}$$

Consider SNAC+ algorithm first. Let $\mathcal{B} = \{\hat{z} = z\}$ be the event that estimated labels in step 1 of the algorithm are consistent with true labels z . By assumption 1, we have $\mathbb{P}(\mathcal{B}^c) \leq \delta_n$. Let $\mathcal{G}_k = \mathcal{C}_k \cap S_2$ and let $\tilde{\rho}_{k\ell}$ be defined as in (18) but with $\hat{\mathcal{G}}_k$ replaced with \mathcal{G}_k . Similarly, let \tilde{T}_n be defined as in (17) but with $\hat{\mathcal{G}}_k$ replaced with \mathcal{G}_k and $\hat{\rho}_{k\ell}$ replaced with $\tilde{\rho}_{k\ell}$. Then, we have $\tilde{T}_n 1_{\mathcal{B}} = \hat{T}_n 1_{\mathcal{B}}$. Applying Lemma 2 multiple times, we obtain

$$\begin{aligned} d_{\mathbb{K}}(\hat{T}_n, Z) &\leq d_{\mathbb{K}}(\hat{T}_n 1_{\mathcal{B}}, Z) + \delta_n \leq \mathbb{E}[d_{\mathbb{K}}(\mathcal{L}(\tilde{T}_n 1_{\mathcal{B}} | \mathcal{F}), Z)] + \delta_n \\ &\leq \mathbb{E}[d_{\mathbb{K}}(\mathcal{L}(\tilde{T}_n | \mathcal{F}), Z)] + 2\delta_n. \end{aligned}$$

Conditioned on \mathcal{F} , $X_{i\ell}(\hat{y})$ is distributed as $\text{Mult}(d_i, \rho_{z_i^*})$ as discussed in (15). We can then apply Theorem 1 (assuming its conditions hold) to the conditional law of \tilde{T}_n given \mathcal{F} to obtain

$$d_{\mathbb{K}}(\mathcal{L}(\tilde{T}_n | \mathcal{F}), Z) \leq \frac{C_{1,\rho}}{\sqrt{L|S_2|}} + \frac{C_{2,\rho}}{h(d)} + \frac{\sqrt{L}}{\underline{\rho}} \left(\sqrt{\frac{32 \log(K_0 \omega_n)}{\omega_n}} + \frac{12K_0 \log(K_0 \omega_n)}{\sqrt{|S_2|}} \right)$$

where $h(d)$ is the harmonic mean of $(d_i, i \in S_2)$, $\omega_n = \min_k \pi_k d_{\text{av}}^{(k)}$ and $d_{\text{av}}^{(k)}$ is the arithmetic average of $(d_i, i \in \mathcal{G}_k)$, $\pi_k = |\mathcal{G}_k|/|S_2|$ and $L = K_0 + 1$. The constants $C_{1,\rho}$ and $C_{2,\rho}$ depend on the ρ matrix defined in (16). Note that $h(d)$ and ω_n , although in general random, are deterministic conditioned on \mathcal{F} . On event \mathcal{A} , as defined in (30), we have

$$\frac{1}{h(d)} = \frac{1}{|S_2|} \sum_{i \in S_2} d_i^{-1} \leq \frac{2}{|S_2|} \sum_{i \in S_2} (d_i^*)^{-1} \leq \frac{4}{C_1 \nu_n}$$

using (32). Since $n_k/n \in [\tau_{\mathcal{C}}, 1]$, and on \mathcal{A} , both $|\mathcal{G}_k|/n_k$ and $|S_2|/n$ belong to $[0.4, 0.6]$, it follows that $\pi_k \in [(2/3)\tau_{\mathcal{C}}, 1.5]$ on \mathcal{A} . Moreover, using (32) and (34), on \mathcal{A} we have,

$$\frac{1}{4} C_1 \nu_n \leq d_{\text{av}}^{(k)} \leq \frac{3}{4} K_0 \nu_n, \quad \forall k \in [K_0],$$

hence $(1/6)\tau_{\mathcal{C}} C_1 \nu_n \leq \omega_n \leq (9/8)K_0 \nu_n$. By the stability assumption on the algorithm that computes \hat{y} , and from (35), we have $\underline{\rho} \geq \tau_{\mathcal{B}} \tau_{\theta} \tau_0 =: \kappa_0$, hence $C_{1,\rho} \geq C_3 - 7$, $C_{2,\rho} \geq C_4/4$ and

$$d_{\mathbb{K}}(\mathcal{L}(\tilde{T}_n | \mathcal{F}), Z) \cdot 1_{\mathcal{A}} \leq \frac{C_3 - 7}{\sqrt{Ln}} + \frac{C_4}{C_1 \nu_n} + \frac{19\sqrt{L}}{\kappa_0} \left(\sqrt{\frac{\alpha_n}{\tau_{\mathcal{C}} C_1 \nu_n}} + \frac{K_0 \alpha_n}{\sqrt{n}} \right) =: \beta_n \quad (37)$$

where $C_3 = 87/\kappa_0^4 + 7$, $C_4 = 4(\pi e)^{-1/2} \max\{1, \kappa_0^{-1} - L - 1\}$ and $\alpha_n = \log((9/8)K_0^2 \nu_n)$ are as defined in the statement of the theorem. The conditions of Theorem 1 hold on \mathcal{A} , if $L \geq 2$, $C_1 \nu_n/4 \geq 2$, $(1/6)\tau_{\mathcal{C}} C_1 \nu_n \geq L$ and $\alpha_n \leq (1/6)\tau_{\mathcal{C}} C_1 \nu_n (\kappa_0/8)^2 n$.

We have $\mathbb{E}[d_{\mathbb{K}}(\mathcal{L}(\tilde{T}_n | \mathcal{F}), Z)] \leq \mathbb{E}[d_{\mathbb{K}}(\mathcal{L}(\tilde{T}_n | \mathcal{F}), Z) \cdot 1_{\mathcal{A}}] + \mathbb{P}(\mathcal{A}^c)$ since the Kolmogorov distance is bounded above by 1. It follows that

$$d_{\mathbb{K}}(\hat{T}_n, Z) \leq \beta_n + 7n^{-1} + 2\delta_n$$

by Lemma 1. Since $\sqrt{nL} \leq n$, we have $(C_3 - 7)/\sqrt{nL} + 7n^{-1} \leq C_3/\sqrt{nL}$ and the result for SNAC+ follows.

For the SNAC algorithm applied with $L = K_0$, we will use the consistency of the column labels \hat{y} instead of the stability assumption. Let $\mathcal{B}_2 = \{\hat{y} = z_{S_1}\}$. By the consistency

assumption, $\mathbb{P}(\mathcal{B}_2^c \mid S_1) \leq \delta_{|S_1|}$. Then, $\mathbb{P}(\mathcal{B}_2^c \mid S_1)1_{\mathcal{A}} \leq \delta_{0.4n}$ hence $\mathbb{P}(\mathcal{B}_2^c) \leq \delta_{0.4n} + \mathbb{P}(\mathcal{A}^c)$. On \mathcal{B}_2 , the confusion matrix R will be diagonal, with diagonal entries $\sum_{j \in \mathcal{C}_k \cap S_1} \theta_j, k \in [K_0]$, hence

$$\rho_{k\ell} = \frac{B_{k\ell}R_{\ell\ell}}{\sum_{\ell'} B_{k\ell'}R_{\ell'\ell'}} \geq \tau_B \tau_\theta \min_{\ell'} \frac{|\mathcal{C}_{\ell'} \cap S_1|}{|S_1|}.$$

On \mathcal{A} , we have $|\mathcal{C}_k \cap S_1|/n_k \in [0.4, 0.6]$ and $|S_1|/n \in [0.4, 0.6]$, hence $|\mathcal{C}_k \cap S_1|/|S_1| \geq (2/3)(n_k/n) \geq (2/3)\tau_{\mathcal{C}}$. Thus, redefining $\kappa_0 = (2/3)\tau_B\tau_\theta\tau_{\mathcal{C}}$, we have $\underline{\rho} \geq \kappa_0$ on $\mathcal{B}_2 \cap \mathcal{A}$. It follows that for the SNAC,

$$d_K(\mathcal{L}(\tilde{T}_n \mid \mathcal{F}), Z) \cdot 1_{\mathcal{A} \cap \mathcal{B}_2} \leq \beta_n$$

with β_n as defined in (37) but with $\kappa_0 = (2/3)\tau_B\tau_\theta\tau_{\mathcal{C}}$ and $L = K_0$. It follows that

$$\begin{aligned} d_K(\hat{T}_n, Z) &\leq \beta_n + 2\delta_n + \mathbb{P}(\mathcal{A}^c \cup \mathcal{B}_2^c) \\ &\leq \beta_n + 2\delta_n + \delta_{0.4n} + 2\mathbb{P}(\mathcal{A}^c). \end{aligned}$$

Since $2\mathbb{P}(\mathcal{A}^c) \leq 14n^{-1}$, we can absorb this term into β_n by redefining \mathcal{C}_3 .

6.2 Proof of Theorem 3

We start by conditioning on \mathcal{F} defined in (28). We recall that conditioned on $d_i, X_{i*}(\hat{y})$ has a multinomial distribution with parameters (d_i, ρ_{z_i*}) where $\rho_{k\ell}$ is defined based on (15) and (16). Let $\xi_{i\ell} = X_{i\ell}(\hat{y})/d_i$ for $i \in S_2$ and note that $\mathbb{E}^{\mathcal{F}}[\xi_{i\ell}] = \rho_{z_i\ell}$ for those i .

Recall that $\hat{\mathcal{C}}_k = \{i : \hat{z}_i = k\}$ and $\hat{n}_k = |\hat{\mathcal{C}}_k|$. For $h \in [K_0]$, a true community \mathcal{C}_h is partitioned into $\hat{\mathcal{C}}_{k,h} = \{i : \hat{z}_i = k, z_i = h\}$, $k \in [K]$. For each $h \in [K_0]$, there exists $k_h \in [K]$ such that $|\hat{\mathcal{C}}_{k_h,h} \cap S_2| \geq |\mathcal{C}_h \cap S_2|/K$. Since $K < K_0$, there are $h_1, h_2 \in [K_0]$ such that $h_1 \neq h_2$ and $k_{h_1} = k_{h_2} = k$. Recalling that $\mathcal{G}_h = \mathcal{C}_h \cap S_2$, on event \mathcal{A} , we have $|\hat{\mathcal{C}}_{k,h_1} \cap S_2| \geq |\mathcal{G}_{h_1}|/K_0 \geq c_1 n$ where $c_1 = 0.4\tau_{\mathcal{C}}/K_0$, and the same goes for $|\hat{\mathcal{C}}_{k,h_2} \cap S_2|$. Therefore, $\hat{\mathcal{C}}_k$ contains ‘‘large’’ pieces of two different true communities $\hat{\mathcal{C}}_{k,h_1}$ and $\hat{\mathcal{C}}_{k,h_2}$. We also have $|\hat{\mathcal{C}}_k \cap S_2| = |\hat{\mathcal{G}}_k| \geq 2c_1 n$. We will focus on $\hat{\mathcal{G}}_k = \hat{\mathcal{C}}_k \cap S_2$ in the following argument.

Let $\bigcup_{r=1}^R \hat{\mathcal{T}}_r$ be a disjoint partition of $\hat{\mathcal{G}}_k$ into the true communities. That is, for each r , there is $h_r \in [K_0]$ such that $\hat{\mathcal{T}}_r = \{i \in S_2 : \hat{z}_i = k, z_i = h_r\} = \hat{\mathcal{C}}_{k,h_r} \cap S_2$, hence $\hat{\mathcal{T}}_r$ lies entirely within true community h_r . For any $i \in \hat{\mathcal{T}}_r$, we have $\mathbb{E}^{\mathcal{F}}[\xi_{i\ell}] = \rho_{h_r\ell}$. Let us define

$$\hat{\alpha}_r = \sum_{i \in \hat{\mathcal{T}}_r} d_i, \quad \hat{\beta}_r := \frac{\hat{\alpha}_r}{\hat{\alpha}_+}, \quad q_{r\ell} := \rho_{h_r\ell}, \quad \bar{q}_\ell := \sum_r \hat{\beta}_r q_{r\ell},$$

where $\hat{\alpha}_+ = \sum_r \hat{\alpha}_r = \sum_{i \in \hat{\mathcal{G}}_k} d_i$. Consider the event

$$\mathcal{E} := \left\{ \max_{i \in \hat{\mathcal{T}}_r} |\xi_{i\ell} - q_{r\ell}| \leq \varepsilon_n := 4\sqrt{\frac{\log n}{C_1 \nu_n}}, \quad \forall r, \ell \right\}. \quad (38)$$

The following lemma shows that \mathcal{E} holds with high probability and we work on \mathcal{E} for the rest of the proof.

Lemma 3. *We have $\mathbb{P}(\mathcal{E}^c \cap \mathcal{A}) \leq 2Ln^{-1}$.*

We next show that $\hat{\rho}_{k\ell}$ is close to \bar{q}_ℓ for all $\ell \in [L]$. We have

$$\begin{aligned} \left| \sum_{i \in \hat{\mathcal{G}}_k} X_{i\ell}(\hat{y}) - \sum_r \hat{\alpha}_r q_{r\ell} \right| &= \left| \sum_r \sum_{i \in \hat{\mathcal{T}}_r} d_i \xi_{i\ell} - \sum_r \sum_{i \in \hat{\mathcal{T}}_r} d_i q_{r\ell} \right| \\ &\leq \sum_r \sum_{i \in \hat{\mathcal{T}}_r} d_i |\xi_{i\ell} - q_{r\ell}| \leq \varepsilon_n \sum_r \hat{\alpha}_r = \varepsilon_n \hat{\alpha}_+. \end{aligned}$$

Dividing by $\hat{\alpha}_+$ and recalling the definition of $\hat{\rho}_{k\ell}$ in (18), we get

$$|\hat{\rho}_{k\ell} - \bar{q}_\ell| = \left| \frac{\sum_{i \in \hat{\mathcal{G}}_k} X_{i\ell}(\hat{y})}{\sum_{i \in \hat{\mathcal{G}}_k} d_i} - \frac{\sum_r \hat{\alpha}_r q_{r\ell}}{\hat{\alpha}_+} \right| \leq \varepsilon_n.$$

We now apply the following lemma:

Lemma 4. *Let $\psi(x, y) = (x - y)^2/y$. Consider (x, y) and (x', y') in $[0, 1] \times [1/c_1, 1]$, where $c_1 > 1$, such that $\max\{|x - x'|, |y - y'|\} \leq \varepsilon \leq 1$. Then,*

$$|\psi(x', y') - \psi(x, y)| \leq 12c_1^3 \varepsilon. \quad (39)$$

Let $\underline{q} = \min_\ell \bar{q}_\ell$. Assuming that $\varepsilon_n \leq \underline{q}/2$ we have $\min\{\hat{\rho}_{k\ell}, \bar{q}_\ell\} \geq \underline{q}/2$, hence we can apply Lemma 4 with $c_1 = 2/\underline{q}$ to obtain

$$|\psi(\xi_{i\ell}, \hat{\rho}_{k\ell}) - \psi(q_{r\ell}, \bar{q}_\ell)| \leq 96\underline{q}^{-3} \varepsilon_n, \quad \forall i \in \hat{\mathcal{T}}_r, \forall \ell \in [L].$$

For two vectors $x, y \in \mathbb{R}^L$, let us write $\Psi(x, y) = \sum_\ell \psi(x_\ell, y_\ell)$. Let $\xi_i = (\xi_{i\ell})$ and $\hat{\rho}_{k*} = (\hat{\rho}_{k\ell})$, and set $\hat{Y}_+^{(u)} = \sum_{i \in \hat{\mathcal{G}}_u} d_i \Psi(\xi_i, \hat{\rho}_{k*})$ for any $u \in [K]$. By the triangle inequality,

$$\hat{Y}_+^{(k)} \geq \sum_r \sum_{i \in \hat{\mathcal{T}}_r} d_i (\Psi(q_{r*}, \bar{q}_*) - 96\underline{q}^{-3} \varepsilon_n L) = \sum_r \hat{\alpha}_r (\Psi(q_{r*}, \bar{q}_*) - 96\underline{q}^{-3} \varepsilon_n L)$$

where $q_{r*} = (q_{r\ell})$ and $\bar{q}_* = (\bar{q}_\ell)$. Dividing by $\hat{\alpha}_+$, we have

$$\frac{1}{\hat{\alpha}_+} \hat{Y}_+^{(k)} \geq \sum_r \hat{\beta}_r \Psi(q_{r*}, \bar{q}_*) - 96\underline{q}^{-3} \varepsilon_n L. \quad (40)$$

Let us define $\omega_1 := \sum_r \hat{\beta}_r \Psi(q_{r*}, \bar{q}_*)$.

Controlling ω_1 and \underline{q} . Recall $|\hat{\mathcal{T}}_1|, |\hat{\mathcal{T}}_2| \geq c_1 n$ and the definition of a_h in (29). On the event \mathcal{A} , for $u = 1, 2$, we have

$$\begin{aligned} \hat{\beta}_u &:= \frac{\sum_{i \in \hat{\mathcal{T}}_u} d_i}{\sum_r \sum_{i \in \hat{\mathcal{T}}_r} d_i} \geq \frac{1}{3} \frac{\sum_{i \in \hat{\mathcal{T}}_u} d_i^*}{\sum_r \sum_{i \in \hat{\mathcal{T}}_r} d_i^*} = \frac{1}{3} \frac{\sum_{i \in \hat{\mathcal{T}}_u} \theta_i a_{h_u}}{\sum_r \sum_{i \in \hat{\mathcal{T}}_r} \theta_i a_{h_r}} \\ &\geq \frac{1}{3} \frac{|\hat{\mathcal{T}}_u| \tau_\theta \theta_{\max} a_{h_u}}{a_{\max} \theta_{\max} |\hat{\mathcal{G}}_k|} \geq \frac{1}{3} \tau_\theta \tau_a c_1 \end{aligned}$$

using $a_h \geq \tau_a a_{\max}$ from (33), $\theta_i \geq \tau_\theta \theta_{\max}$ and $|\hat{\mathcal{G}}_k| \leq n$. Rearranging, we have

$$\omega_1 = \sum_r \hat{\beta}_r \sum_\ell \frac{(q_{r\ell} - \bar{q}_\ell)^2}{\bar{q}_\ell} = \sum_\ell \frac{1}{\bar{q}_\ell} \sum_r \hat{\beta}_r (q_{r\ell} - \bar{q}_\ell)^2.$$

The inner summation is the variance of a random variable taking values $\{q_{r\ell}\}$ with probabilities $\{\hat{\beta}_r\}$. Applying Lemma 11 in the Supplement (Section C) and recalling the definition of ω_2 from (41), we have

$$\omega_1 \geq \frac{1}{\max_{\ell} \bar{q}_{\ell}} \frac{1}{2} \hat{\beta}_1 \hat{\beta}_2 \sum_{\ell} (q_{1\ell} - q_{2\ell})^2 \geq \frac{1}{18} \tau_{\theta}^2 \tau_a^2 c_1^2 \|q_{1*} - q_{2*}\|^2 \geq L\omega_2 \quad (41)$$

since $\max_{\ell} \bar{q}_{\ell} \leq \max_{k,\ell} \rho_{k\ell} \leq 1$. To identify \underline{q} , recall $\underline{\rho} \geq \tau_B \tau_{\theta} \tau_0 =: \tau_{\rho}$ from (35); then

$$\bar{q}_{\ell} \geq \sum_{r=1,2} \hat{\beta}_r q_{r\ell} \geq \frac{2}{3} c_1 \tau_{\theta} \tau_a \underline{\rho} \geq \frac{2}{3} c_1 \tau_{\theta} \tau_a \tau_{\rho} = \underline{q}.$$

Putting the pieces together. On Ω_n , we have $96\underline{q}^{-3}\varepsilon_n \leq \frac{1}{2}\omega_2$, which combined with (41) ($\omega_1 \geq L\omega_2$) and (40), gives $\frac{1}{\hat{\alpha}_+} \hat{Y}_+^{(k)} \geq \frac{1}{2}L\omega_2$. Recall that, on \mathcal{A} , $|\hat{g}_k| \geq 2c_1n$ and $d_i \geq C_1\nu_n/4$. Then, on $\Omega_n \cap \mathcal{E} \cap \mathcal{A}$,

$$\hat{Y}_+^{(k)} \geq \frac{1}{4}c_1C_1L\omega_2n\nu_n.$$

Furthermore, $\tilde{n} = |S_2| \leq 0.6n$ on \mathcal{A} , hence $\gamma_{\tilde{n}} = \sqrt{\tilde{n}(L-1)} \leq \sqrt{0.6nL}$ and we have

$$\begin{aligned} \hat{T}_n &= \frac{1}{\sqrt{2}} \left(\frac{1}{\gamma_{\tilde{n}}} \sum_{u=1}^K \hat{Y}_+^{(u)} - \gamma_{\tilde{n}} \right) \geq \frac{1}{\sqrt{2}} \left(\frac{1}{\gamma_{\tilde{n}}} \hat{Y}_+^{(k)} - \gamma_{\tilde{n}} \right) \\ &\geq \sqrt{\frac{n}{2}} \left(\frac{c_1C_1L\omega_2\nu_n/4}{\sqrt{0.6L}} - \sqrt{0.6L} \right). \end{aligned}$$

By assumption $\frac{1}{2}(c_1C_1L\omega_2\nu_n/4) \geq 0.6L$, hence on $\Omega_n \cap \mathcal{E} \cap \mathcal{A}$, we obtain

$$\hat{T}_n \geq \sqrt{\frac{n}{2}} \left(\frac{c_1C_1L\omega_2\nu_n/8}{\sqrt{0.6L}} \right) \geq \frac{c_1C_1}{10} \omega_2 \nu_n \sqrt{Ln}.$$

Finally, we note that

$$\mathbb{P}((\Omega_n \cap \mathcal{E} \cap \mathcal{A})^c) \leq \mathbb{P}(\Omega^c) + 2Ln^{-1} + 2(7n^{-1}) \leq \mathbb{P}(\Omega^c) + 9Ln^{-1}$$

using Lemmas 1 and 3 and $L \geq 2$. The proof of Theorem 3 is complete.

Acknowledgement

This work was supported in part by NSF CAREER grant DMS-1945667. We thank Mason Porter who provided access to the Facebook-100 dataset.

References

- [Abb18] E. Abbe. Community Detection and Stochastic Block Models: Recent Developments. *Journal of Machine Learning Research* 18.177 (2018), pp. 1–86.

- [Abb+20] E. Abbe, J. Fan, K. Wang, Y. Zhong, et al. Entrywise eigenvector analysis of random matrices with low expected rank. *Annals of Statistics* 48.3 (2020), pp. 1452–1474.
- [ABH16] E. Abbe, A. S. Bandeira, and G. Hall. Exact Recovery in the Stochastic Block Model. *IEEE Transactions on Information Theory* 62.1 (2016), pp. 471–487.
- [AG05] L. A. Adamic and N. Glance. The Political Blogosphere and the 2004 U.S. Election: Divided They Blog. *Proceedings of the 3rd International Workshop on Link Discovery*. LinkKDD '05. Chicago, Illinois: Association for Computing Machinery, 2005, 36–43.
- [AH10] S. Anders and W. Huber. Differential expression analysis for sequence count data. *Genome Biology* 11.10 (2010), R106.
- [AL18] A. A. Amini and E. Levina. On semidefinite relaxations for the block model. *Ann. Statist.* 46.1 (Feb. 2018), pp. 149–179.
- [Ami+13] A. A. Amini, A. Chen, P. J. Bickel, and E. Levina. Pseudo-likelihood methods for community detection in large sparse networks. *Ann. Statist.* 41.4 (Aug. 2013), pp. 2097–2122.
- [AS15] E. Abbe and C. Sandon. Detection in the stochastic block model with multiple clusters: proof of the achievability conjectures, acyclic BP, and the information-computation gap. *arXiv preprint arXiv:1512.09080* (2015).
- [BC09] P. J. Bickel and A. Chen. A nonparametric view of network models and Newman–Girvan and other modularities. *Proceedings of the National Academy of Sciences* 106.50 (2009), pp. 21068–21073. eprint: <https://www.pnas.org/content/106/50/21068.full.pdf>.
- [Bic+13] P. Bickel, D. Choi, X. Chang, and H. Zhang. Asymptotic normality of maximum likelihood and its variational approximation for stochastic blockmodels. *Ann. Statist.* 41.4 (Aug. 2013), pp. 1922–1943.
- [Bre01] L. Breiman. Statistical Modeling: The Two Cultures (with comments and a rejoinder by the author). *Statist. Sci.* 16.3 (Aug. 2001), pp. 199–231.
- [BRS06] P. J. Bickel, Y. Ritov, and T. M. Stoker. Tailor-made tests for goodness of fit to semiparametric hypotheses. *Ann. Statist.* 34.2 (Apr. 2006), pp. 721–741.
- [BS16] P. J. Bickel and P. Sarkar. Hypothesis testing for automated community detection in networks. *Journal of the Royal Statistical Society: Series B (Statistical Methodology)* 78.1 (2016), pp. 253–273. eprint: <https://rss.onlinelibrary.wiley.com/doi/pdf/10.1111/rssb.12117>.
- [CCT12] K. Chaudhuri, F. Chung, and A. Tsias. Spectral clustering of graphs with general degrees in the extended planted partition model. *Conference on Learning Theory*. 2012, pp. 35–1.
- [CL18] K. Chen and J. Lei. Network Cross-Validation for Determining the Number of Communities in Network Data. *Journal of the American Statistical Association* 113.521 (2018), pp. 241–251. eprint: <https://doi.org/10.1080/01621459.2016.1246365>.

- [CRV15] P. Chin, A. Rao, and V. Vu. Stochastic Block Model and Community Detection in Sparse Graphs: A spectral algorithm with optimal rate of recovery. Ed. by P. Grünwald, E. Hazan, and S. Kale. Vol. 40. Proceedings of Machine Learning Research. Paris, France: PMLR, 2015, pp. 391–423.
- [Dec+11] A. Decelle, F. Krzakala, C. Moore, and L. Zdeborová. Asymptotic analysis of the stochastic block model for modular networks and its algorithmic applications. *Phys. Rev. E* 84 (6 2011), p. 066106.
- [DPR08] J.-J. Daudin, F. Picard, and S. Robin. A mixture model for random graphs. *Statistics and computing* 18.2 (2008), pp. 173–183.
- [EYY12] L. Erdős, H.-T. Yau, and J. Yin. Rigidity of eigenvalues of generalized Wigner matrices. *Advances in Mathematics* 229.3 (2012), pp. 1435–1515.
- [FC19] Y. Fei and Y. Chen. Achieving the Bayes Error Rate in Stochastic Block Model by SDP, Robustly. Ed. by A. Beygelzimer and D. Hsu. Vol. 99. Proceedings of Machine Learning Research. Phoenix, USA: PMLR, 2019, pp. 1235–1269.
- [Fis+13] D. E. Fishkind et al. Consistent Adjacency-Spectral Partitioning for the Stochastic Block Model When the Model Parameters Are Unknown. *SIAM Journal on Matrix Analysis and Applications* 34.1 (2013), pp. 23–39. eprint: <https://doi.org/10.1137/120875600>.
- [Gao+17] C. Gao, Z. Ma, A. Y. Zhang, and H. H. Zhou. Achieving optimal misclassification proportion in stochastic block models. *The Journal of Machine Learning Research* 18.1 (2017), pp. 1980–2024.
- [Gao+18] C. Gao, Z. Ma, A. Y. Zhang, and H. H. Zhou. Community detection in degree-corrected block models. *Ann. Statist.* 46.5 (Oct. 2018), pp. 2153–2185.
- [GBP19] J. Geng, A. Bhattacharya, and D. Pati. Probabilistic Community Detection With Unknown Number of Communities. *Journal of the American Statistical Association* 114.526 (2019), pp. 893–905. eprint: <https://doi.org/10.1080/01621459.2018.1458618>.
- [GHW79] G. H. Golub, M. Heath, and G. Wahba. Generalized cross-validation as a method for choosing a good ridge parameter. *Technometrics* 21.2 (1979), pp. 215–223.
- [GN15] E. Giné and R. Nickl. *Mathematical Foundations of Infinite-Dimensional Statistical Models*. Cambridge Series in Statistical and Probabilistic Mathematics. Cambridge University Press, 2015.
- [HGH08] D. R. Hunter, S. M. Goodreau, and M. S. Handcock. Goodness of fit of social network models. *Journal of the American Statistical Association* 103.481 (2008), pp. 248–258.
- [HLL83] P. W. Holland, K. B. Laskey, and S. Leinhardt. Stochastic blockmodels: First steps. 1983.
- [HO93] P. C. Hansen and D. P. O’Leary. The use of the L-curve in the regularization of discrete ill-posed problems. *SIAM journal on scientific computing* 14.6 (1993), pp. 1487–1503.

- [Hu+19] J. Hu, H. Qin, T. Yan, and Y. Zhao. Corrected Bayesian Information Criterion for Stochastic Block Models. *Journal of the American Statistical Association* 0.0 (2019), pp. 1–13. eprint: <https://doi.org/10.1080/01621459.2019.1637744>.
- [HW08] J. M. Hofman and C. H. Wiggins. Bayesian approach to network modularity. *Physical review letters* 100.25 (2008), p. 258701.
- [JY16] A. Joseph and B. Yu. Impact of regularization on spectral clustering. *Ann. Statist.* 44.4 (Aug. 2016), pp. 1765–1791.
- [Kar+16] V. Karwa et al. Exact tests for stochastic block models. *arXiv preprint arXiv:1612.06040* (2016).
- [KK17] T. Kawamoto and Y. Kabashima. Cross-validation estimate of the number of clusters in a network. *Scientific Reports* 7.1 (2017).
- [KN11] B. Karrer and M. E. J. Newman. Stochastic blockmodels and community structure in networks. *Phys. Rev. E* 83 (1 Jan. 2011), p. 016107.
- [Krz+13] F. Krzakala et al. Spectral redemption in clustering sparse networks. *Proceedings of the National Academy of Sciences* 110.52 (2013), pp. 20935–20940. eprint: <https://www.pnas.org/content/110/52/20935.full.pdf>.
- [LC13] Y. Li and K. C. Carriere. Assessing goodness of fit of exponential random graph models. *International Journal of Statistics and Probability* 2.4 (2013), p. 64.
- [LCX18] X. Li, Y. Chen, and J. Xu. Convex relaxation methods for community detection. *arXiv preprint arXiv:1810.00315* (2018).
- [Lei16] J. Lei. A goodness-of-fit test for stochastic block models. *Ann. Statist.* 44.1 (Feb. 2016), pp. 401–424.
- [LL15] C. M. Le and E. Levina. *Estimating the number of communities in networks by spectral methods*. 2015. arXiv: [1507.00827](https://arxiv.org/abs/1507.00827) [stat.ML].
- [LLV17] C. M. Le, E. Levina, and R. Vershynin. Concentration and regularization of random graphs. *Random Structures & Algorithms* 51.3 (2017), pp. 538–561. eprint: <https://onlinelibrary.wiley.com/doi/pdf/10.1002/rsa.20713>.
- [LLZ20] T. Li, E. Levina, and J. Zhu. Network cross-validation by edge sampling. *Biometrika* 107.2 (Apr. 2020), pp. 257–276. eprint: <https://academic.oup.com/biomet/article-pdf/107/2/257/33218033/asaa006.pdf>.
- [LR15] J. Lei and A. Rinaldo. Consistency of spectral clustering in stochastic block models. *Ann. Statist.* 43.1 (Feb. 2015), pp. 215–237.
- [LY+14] J. O. Lee, J. Yin, et al. A necessary and sufficient condition for edge universality of Wigner matrices. *Duke Mathematical Journal* 163.1 (2014), pp. 117–173.
- [LZ17] J. Lei and L. Zhu. Generic Sample Splitting For Refined Community Recovery In Degree Corrected Stochastic Block Models. *Statistica Sinica* 27.4 (2017), pp. 1639–1659.
- [MNS16a] E. Mossel, J. Neeman, and A. Sly. Belief propagation, robust reconstruction and optimal recovery of block models. *Ann. Appl. Probab.* 26.4 (Aug. 2016), pp. 2211–2256.

- [MNS16b] E. Mossel, J. Neeman, and A. Sly. Consistency thresholds for binary symmetric block models. *Electronic Journal of Probability* 21 (2016).
- [MS12] M. Mørup and M. N. Schmidt. Bayesian Community Detection. *Neural Computation* 24.9 (2012). PMID: 22509971, pp. 2434–2456. eprint: https://doi.org/10.1162/NECO_a_00314.
- [MSZ18] S. Ma, L. Su, and Y. Zhang. Determining the Number of Communities in Degree-corrected Stochastic Block Models. *arXiv preprint arXiv:1809.01028* (2018).
- [NG04] M. E. Newman and M. Girvan. Finding and Evaluating Community Structure in Networks. *Physical review. E, Statistical, nonlinear, and soft matter physics* 69 (Mar. 2004), p. 026113.
- [NR16] M. E. Newman and G. Reinert. Estimating the number of communities in a network. *Physical review letters* 117.7 (2016), p. 078301.
- [OFDR19] L. Ospina-Forero, C. M. Deane, and G. Reinert. Assessment of model fit via network comparison methods based on subgraph counts. *Journal of Complex Networks* 7.2 (2019), pp. 226–253.
- [PAL19] M. S. Paez, A. A. Amini, and L. Lin. Hierarchical stochastic block model for community detection in multiplex networks. *arXiv preprint arXiv:1904.05330* (2019).
- [PV18] S. L. van der Pas and A. W. van der Vaart. Bayesian Community Detection. *Bayesian Anal.* 13.3 (Sept. 2018), pp. 767–796.
- [QR13] T. Qin and K. Rohe. Regularized spectral clustering under the degree-corrected stochastic blockmodel. *Advances in neural information processing systems*. 2013, pp. 3120–3128.
- [RCY11] K. Rohe, S. Chatterjee, and B. Yu. Spectral clustering and the high-dimensional stochastic blockmodel. *Ann. Statist.* 39.4 (Aug. 2011), pp. 1878–1915.
- [Rio+17] M. A. Riolo, G. T. Cantwell, G. Reinert, and M. E. Newman. Efficient method for estimating the number of communities in a network. *Physical review e* 96.3 (2017), p. 032310.
- [She10] I. Shevtsova. An Improvement of Convergence Rate Estimates in the Lyapunov Theorem. *Doklady Mathematics* 82 (Dec. 2010), pp. 862–864.
- [SKZ14] A. Saade, F. Krzakala, and L. Zdeborová. Spectral Clustering of graphs with the Bethe Hessian. *Advances in Neural Information Processing Systems 27*. Ed. by Z. Ghahramani et al. Curran Associates, Inc., 2014, pp. 406–414.
- [SN97] T. A. Snijders and K. Nowicki. Estimation and prediction for stochastic blockmodels for graphs with latent block structure. *Journal of classification* 14.1 (1997), pp. 75–100.
- [Suw+16] S. Suwan et al. Empirical Bayes estimation for the stochastic blockmodel. *Electron. J. Statist.* 10.1 (2016), pp. 761–782.
- [TMP12] A. L. Traud, P. J. Mucha, and M. A. Porter. Social structure of Facebook networks. *Physica A: Statistical Mechanics and its Applications* 391.16 (2012), pp. 4165–4180.

- [Tra+11] A. L. Traud, E. D. Kelsic, P. J. Mucha, and M. A. Porter. Comparing community structure to characteristics in online collegiate social networks. *SIAM review* 53.3 (2011), pp. 526–543.
- [Vaa98] A. W. v. d. Vaart. *Asymptotic Statistics*. Cambridge Series in Statistical and Probabilistic Mathematics. Cambridge University Press, 1998.
- [WB17] Y. X. R. Wang and P. J. Bickel. Likelihood-based model selection for stochastic block models. *Ann. Statist.* 45.2 (Apr. 2017), pp. 500–528.
- [Yan+14a] X. Yan et al. Model selection for degree-corrected block models. *Journal of Statistical Mechanics: Theory and Experiment* 2014.5 (2014), P05007.
- [Yan+14b] X. Yan et al. Model selection for degree-corrected block models. *Journal of Statistical Mechanics: Theory and Experiment* 2014.5 (May 2014), P05007.
- [Yan16] X. Yan. Bayesian model selection of stochastic block models. *2016 IEEE/ACM International Conference on Advances in Social Networks Analysis and Mining (ASONAM)*. 2016, pp. 323–328.
- [YFS18] M. Yuan, Y. Feng, and Z. Shang. *A likelihood-ratio type test for stochastic block models with bounded degrees*. 2018. arXiv: [1807.04426](https://arxiv.org/abs/1807.04426) [stat.ME].
- [YP14] S.-Y. Yun and A. Proutiere. Accurate community detection in the stochastic block model via spectral algorithms. *arXiv preprint arXiv:1412.7335* (2014).
- [YSC18] B. Yan, P. Sarkar, and X. Cheng. Provable Estimation of the Number of Blocks in Block Models. *Proceedings of the Twenty-First International Conference on Artificial Intelligence and Statistics*. Ed. by A. Storkey and F. Perez-Cruz. Vol. 84. Proceedings of Machine Learning Research. Playa Blanca, Lanzarote, Canary Islands: PMLR, 2018, pp. 1185–1194.
- [ZA19] Z. Zhou and A. A. Amini. Analysis of spectral clustering algorithms for community detection: the general bipartite setting. *J. Mach. Learn. Res.* 20 (2019), pp. 47–1.
- [ZA20a] L. Zhang and A. A. Amini. *Adjusted chi-square test for degree-corrected block models: Experiments in R*. <https://github.com/linfanz/nac-test>. 2020.
- [ZA20b] Z. Zhou and A. A. Amini. Optimal Bipartite Network Clustering. *Journal of Machine Learning Research* 21.40 (2020), pp. 1–68.
- [ZLZ12] Y. Zhao, E. Levina, and J. Zhu. Consistency of community detection in networks under degree-corrected stochastic block models. *Ann. Statist.* 40.4 (Aug. 2012), pp. 2266–2292.
- [ZM14] P. Zhang and C. Moore. Scalable detection of statistically significant communities and hierarchies, using message passing for modularity. *Proceedings of the National Academy of Sciences* 111.51 (2014), pp. 18144–18149. eprint: <https://www.pnas.org/content/111/51/18144.full.pdf>.
- [ZR18] Y. Zhang and K. Rohe. Understanding regularized spectral clustering via graph conductance. *Advances in Neural Information Processing Systems*. 2018, pp. 10631–10640.
- [ZZ20] A. Y. Zhang and H. H. Zhou. Theoretical and computational guarantees of mean field variational inference for community detection. *Ann. Statist.* 48.5 (Oct. 2020), pp. 2575–2598.

The Supplement to “Adjusted chi-square test for degree-corrected block models”

Linfan Zhang and Arash A. Amini

This supplement collects the remaining proofs and additional empirical results.

A Proof of Theorem 1

The result follows by combining the following two propositions:

Proposition 1. *Let $X_i \sim \text{Mult}(d_i, p_{k^*})$, $i \in \mathcal{G}_k, k \in [K]$ be independent L -dimensional multinomial variables, with probability vectors $p_{k^*} = (p_{k\ell})$, and let*

$$Y_i := \sum_{\ell=1}^L \psi(X_{i\ell}, d_i p_{g_i, \ell}) \quad \text{and} \quad S_n = \frac{1}{v_n} \sum_{i=1}^n (Y_i - \mathbb{E}[Y_i])$$

where $v_n^2 := \sum_{i=1}^n \text{var}(Y_i)$. Moreover, let $T_n = \frac{1}{\sqrt{2\gamma_n}} (\sum_{i=1}^n Y_i - \gamma_n^2)$ where $\gamma_n = \sqrt{n(L-1)}$. Let $\underline{p} = \min_{k, \ell} p_{k\ell}$ and assume that $\min\{h(d), L\} \geq 2$. Then, with $Z \sim N(0, 1)$, we have

$$d_K(S_n, Z) \leq \frac{55}{\underline{p}^4 \sqrt{Ln}}, \quad (42)$$

$$d_K(T_n, Z) \leq d_K(S_n, Z) + \frac{\max\{1, \underline{p}^{-1} - L - 1\}}{\sqrt{\pi e}} h(d)^{-1}. \quad (43)$$

Proposition 2. *Recall that $\omega_n = \min_k \pi_k d_{av}^{(k)}$. Under the assumptions of Theorem 1, for any nonnegative $u \leq (\underline{p}/8)^2 n \omega_n$, we have*

$$d_K(\widehat{T}_n, Z) \leq d_K(T_n, Z) + \frac{\sqrt{L}}{\underline{p}} \left[\sqrt{\frac{8u}{\omega_n}} + 12K \frac{u}{\sqrt{n}} \right] + 2KLe^{-u}. \quad (44)$$

To obtain (11) in Theorem 1, we take $u = \log(K\omega_n)$. To satisfy the condition of Proposition 2, we need $\log(K\omega_n)/\omega_n \leq (\underline{p}/8)^2 n$. Since $\omega_n \geq L \geq 2$ by assumption and thus $2 \log(K\omega_n) \geq 1$, we have

$$2KLe^{-u} = 2L/\omega_n \leq \frac{1}{\underline{p}} \sqrt{8L \log(K\omega_n)/\omega_n} = \frac{1}{\underline{p}} \sqrt{8Lu/\omega_n},$$

and the result follows.

A.1 Proof of Proposition 1

We first introduce two lemmas used in the proof of Proposition 1. Lemma 5 is on the mean and variance of the chi-square statistic. Lemma 6 is a general result on the growth rate of the third central moment of the empirical variance of a sum of independent variables. Applying this result to a chi-square statistic, we can bound its third central moment by some constant. Recall that $\psi(x, y) := (x - y)^2/y$.

Lemma 5 (Variance of the chi-square statistic). *Let $X = (X_1, \dots, X_L) \sim \text{Mult}(d, p)$, where $p = (p_1, \dots, p_L)$ is a probability vector and let $Y := \sum_{\ell=1}^L \psi(X_\ell, dp_\ell)$. Then, for $L \geq 2$,*

$$\begin{aligned}\mathbb{E}[Y] &= L - 1, \\ \text{var}(Y) &= \left(1 - \frac{1}{d}\right)2(L - 1) + \frac{1}{d}\left(\frac{L}{h(p)} - L^2\right).\end{aligned}$$

In particular, $\text{var}(Y) \geq (1 - 1/d)2(L - 1)$

Note that we always have $L/h(p) \geq L^2$ since $\sum_{\ell} p_\ell = 1$. Hence, the variance of Y is a convex combination of two nonnegative terms. Furthermore, if $d \geq 2$, $\text{var}(Y) \geq L - 1$.

Lemma 6 (Central moment growth). *Let $\{W_1, \dots, W_n\}$ be a sequence of i.i.d. zero mean random variables with finite moments of order 6, and let $X_n = \sum_{i=1}^n W_i$. Then, the third central moment of X_n^2 is $O(n^3)$:*

$$\mathbb{E}|X_n^2 - \mathbb{E}X_n^2|^3 \leq C_{W_1} n^3,$$

where C_{W_1} is a constant that only depends on the first 6 moments of W_1 . For the case where $W_1 = \alpha(Z - p)$ with $Z \sim \text{Ber}(p)$ and $\alpha \in \mathbb{R}$, one can take $C_{W_1} = 34.5 \alpha^6 p(1 - p)$.

Proof Proposition 1. By Esseen's bound for non-identically distributed summands [She10],

$$d_K(S_n, Z) \leq \frac{C_0}{(v_n^2)^{3/2}} \sum_{i=1}^n \mathbb{E}|Y_i - \mathbb{E}[Y_i]|^3 \quad (45)$$

for some constant $C_0 \in [0.41, 0.56]$. By Lemma 5, $\text{var}(Y_i) \geq (1 - d_i^{-1})2(L - 1)$. Then, using assumption $h(d) \geq 2$,

$$v_n^2 = \sum_{i=1}^n \text{var}(Y_i) \geq n(1 - h(d)^{-1})2(L - 1) \geq n(L - 1). \quad (46)$$

Next, we bound the third central moment of Y_i . Let $Z_{i\ell} = (X_{i\ell} - d_i p_{g_i\ell})/p_{g_i\ell}$. We have $Y_i = \sum_{\ell} p_{g_i\ell} Z_{i\ell}^2/d_i$. We can write $Z_{i\ell} = \sum_{j=1}^{d_i} (W_j - p_{g_i\ell})/p_{g_i\ell}$, where $W_j \stackrel{i.i.d.}{\sim} \text{Ber}(p_{g_i\ell})$. By Lemma 6, $\mathbb{E}|Z_{i\ell}^2 - \mathbb{E}Z_{i\ell}^2|^3 \leq C_{p_{g_i\ell}} d_i^3$, for some constant $C_{p_{g_i\ell}}$ that only depends on $p_{g_i\ell}$. Then,

$$\begin{aligned}\mathbb{E}|Y_i - \mathbb{E}[Y_i]|^3 &= \mathbb{E}\left|\sum_{\ell=1}^L p_{g_i\ell}(Z_{i\ell}^2 - \mathbb{E}Z_{i\ell}^2)/d_i\right|^3 \\ &\leq \sum_{\ell=1}^L \frac{p_{g_i\ell}}{d_i^3} \mathbb{E}|Z_{i\ell}^2 - \mathbb{E}Z_{i\ell}^2|^3 \leq \sum_{\ell=1}^L p_{g_i\ell} \left(\frac{34.5}{p_{g_i\ell}^6} p_{g_i\ell}(1 - p_{g_i\ell})\right)\end{aligned} \quad (47)$$

where the first inequality is the discrete Jensen's inequality applied to convex function $x \mapsto |x|^3$, that is, $|\sum_{\ell} q_\ell x_\ell|^3 \leq \sum_{\ell} q_\ell |x_\ell|^3$ for any $\{x_\ell\}$ and probability vector $q = (q_\ell)$. Combining (45), (46) and (47) gives

$$\sqrt{n} d_K(S_n, Z) \leq \frac{34.5C_0}{(L - 1)^{3/2}} \frac{1}{n} \sum_{i=1}^n \sum_{\ell=1}^L \frac{1}{p_{g_i\ell}^4} \leq 34.5C_0 2^{3/2} \frac{1}{L^{1/2} \underline{p}^4} \leq \frac{55}{L^{1/2} \underline{p}^4}$$

using $p_{g_i\ell} \geq \underline{p}$ for all i and ℓ , $L - 1 \geq L/2$ and $C_0 \leq 0.56$.

To prove (43), let $\beta_n = v_n/(\sqrt{2}\gamma_n)$, so that $T_n = \beta_n S_n$. By Lemma 9,

$$d_K(T_n, Z) \leq d_K(S_n, Z) + \frac{\zeta_n}{\sqrt{2\pi e}}, \quad \zeta_n := \frac{|\beta_n - 1|}{\min\{\beta_n, 1\}}.$$

It remains to bound ζ_n . Let $d_{\mathcal{G}_k} = (d_i, i \in \mathcal{G}_k)$ and $n_k = |\mathcal{G}_k|$. By Lemma 5,

$$\begin{aligned} v_n^2 &= \sum_{i=1}^n (1 - d_i^{-1})2(L - 1) + d_i^{-1}(Lh(p_{g_i^*})^{-1} - L^2) \\ &= \sum_k n_k \left[(1 - h(d_{\mathcal{G}_k})^{-1})2(L - 1) + h(d_{\mathcal{G}_k})^{-1}(Lh(p_{k^*}) - L^2) \right] \end{aligned}$$

where the second line follows by breaking the sum as $\sum_{i=1}^n (\dots) = \sum_{k=1}^K \sum_{i \in \mathcal{G}_k} (\dots)$ and using $n_k h(d_{\mathcal{G}_k})^{-1} = \sum_{i \in \mathcal{G}_k} d_i^{-1}$. To simplify, let $\alpha_k = h(d_{\mathcal{G}_k})^{-1}$. Then,

$$\beta_n = \frac{v_n}{\sqrt{2}\gamma_n} = \left(\sum_k \pi_k (1 + \alpha_k b_k) \right)^{1/2}, \quad b_k := \frac{Lh(p_{k^*})^{-1} - L^2}{2(L - 1)} - 1.$$

where $\pi_k = n_k/n$. Since $L \leq h(p_{k^*})^{-1} \leq \underline{p}^{-1}$ and $L/2 \leq L - 1$, we have

$$0 \leq b_k + 1 \leq \frac{L(\underline{p}^{-1} - L)}{2(L - 1)} \leq \underline{p}^{-1} - L. \quad (48)$$

Let $u = \sum_k \pi_k \alpha_k b_k$ and note that $\beta_n = \sqrt{1 + u}$. We have $0 < \sum_k \pi_k \alpha_k = h(d)^{-1} \leq 1/2$, by assumption. Moreover $b_k \geq -1$ for all k from (48). It follows that $u \geq -1/2$.

If $u \geq 0$, then $\beta_n \geq 1$ and $\zeta_n = \beta_n - 1 \leq \frac{1}{2}u$, using the inequality $\sqrt{1+x} \leq 1 + x/2$ which holds for all $x \geq -1$. If $u < 0$, then $\beta_n \in (0, 1)$, and

$$\zeta_n = \frac{1}{\beta_n} - 1 = \frac{1}{\sqrt{1 - |u|}} - 1 \leq \sqrt{2}|u|,$$

using $|u| \leq 1/2$ and the inequality $(1 - x)^{-1/2} \leq 1 + \sqrt{2}x$ which holds for $0 \leq x \leq 0.77$. We have $|b_k| \leq \max\{1, \underline{p}^{-1} - L - 1\}$, hence $\zeta_n \leq \sqrt{2} \max\{1, \underline{p}^{-1} - L - 1\} h(d)^{-1}$. The proof is complete. \square

A.2 Proof of Proposition 2

We need the following technical lemmas:

Lemma 7. *Let $x = (x_1, \dots, x_n) \in \mathbb{R}^d$ and $y, y + v \in \mathbb{R} \setminus \{0\}$, and consider the function $G(v) = \sum_{i=1}^n d_i \psi(x_i, y + v)$ where $\{d_i\}$ are nonnegative and $\psi(s, t) = (s - t)^2/t$. Let $R = \sum_i d_i x_i - d_+ y$ where $d_+ = \sum_{i=1}^n d_i$, and assume further that $|v| \leq |y|/2$. Then,*

$$|G(v) - G(0)| \leq \frac{2|v|}{|y|} [G(0) + 2|R| + |v|d_+].$$

Lemma 8. Let $\delta \in [0, 1/2]$ and $\varepsilon > 0$. Then, for any two random variables \widehat{T}_n and T_n , and $Z \sim N(0, 1)$

$$d_K(\widehat{T}_n, Z) \leq d_K(T_n, Z) + \frac{1}{2}(\delta + \varepsilon) + \mathbb{P}(|\widehat{T}_n - T_n| \geq \delta T_n + \varepsilon).$$

Let $X_{+\ell}^{(k)} = \sum_{i \in \mathcal{G}_k} X_{i\ell}$ and $d_+^{(k)} = \sum_{i \in \mathcal{G}_k} d_i$. We note that $d_+^{(k)} \widehat{\Delta}_{k\ell}$ is a centered Bin($d_+^{(k)}, p_{k\ell}$) variable. Applying Proposition 4 (Section C), we have

$$\mathbb{P}\left(|\widehat{\Delta}_{k\ell}| \geq \sqrt{\frac{2u}{d_+^{(k)}}} + \frac{u}{3d_+^{(k)}}\right) \leq 2e^{-u}.$$

To simplify, let $\alpha := \min_k d_+^{(k)}$. Assuming that $u \leq d_+^{(k)}$ for all k , that is, $u \leq \alpha$, the event

$$\mathcal{B} := \left\{ \max_{\ell} |\widehat{\Delta}_{k\ell}| \leq 2(u/d_+^{(k)})^{1/2} =: \delta_k, \forall k \in [K] \right\} \quad (49)$$

holds with probability at least $1 - 2KLe^{-u}$. Let $\delta := \max_k \delta_k = 2\sqrt{u/\alpha}$. For the rest of the proof, we work on \mathcal{B} .

We now apply Lemma 7 with $x_i = X_{i\ell}/d_i$, $y = p_{k\ell}$ and $v = \widehat{p}_{k\ell} - p_{k\ell} =: \widehat{\Delta}_{k\ell}$. Note the condition $|v| \leq |y|/2$ of the lemma is satisfied on \mathcal{B} , as long as $\delta \leq \underline{p}/2$. Let

$$G_{k\ell}(\widehat{\Delta}_{k\ell}) = \sum_{i \in \mathcal{G}_k} d_i \psi(X_{i\ell}/d_i, p_{k\ell} + \widehat{\Delta}_{k\ell}).$$

We have $\sqrt{2}\gamma_n \widehat{T}_n = \sum_{k,\ell} G_{k\ell}(\widehat{\Delta}_{k\ell}) - \gamma_n^2$ and $\sqrt{2}\gamma_n T_n = \sum_{k,\ell} G_{k\ell}(0) - \gamma_n^2$, hence

$$\begin{aligned} \sqrt{2}\gamma_n |\widehat{T}_n - T_n| &\leq \sum_{k,\ell} |G_{k\ell}(\widehat{\Delta}_{k\ell}) - G_{k\ell}(0)| \\ &\leq 2 \sum_{k,\ell} \frac{|\widehat{\Delta}_{k\ell}|}{p_{k\ell}} \left[G_{k\ell}(0) + 2|X_{+\ell}^{(k)} - d_+^{(k)} p_{k\ell}| + |\widehat{\Delta}_{k\ell}| d_+^{(k)} \right] \\ &= 2 \sum_{k,\ell} \frac{|\widehat{\Delta}_{k\ell}|}{p_{k\ell}} \left[G_{k\ell}(0) + 3|\widehat{\Delta}_{k\ell}| d_+^{(k)} \right] \end{aligned}$$

where we have used $X_{+\ell}^{(k)} - d_+^{(k)} p_{k\ell} = d_+^{(k)} \widehat{\Delta}_{k\ell}$ since $\widehat{p}_{k\ell} = X_{+\ell}^{(k)}/d_+^{(k)}$. By assumption $p_{k\ell} \geq \underline{p}$ for all k and ℓ . Hence,

$$\sqrt{2}\gamma_n |\widehat{T}_n - T_n| \leq \frac{2}{\underline{p}} \left[\delta \sum_{k,\ell} G_{k\ell}(0) + 3L \sum_k \delta_k^2 d_+^{(k)} \right] = \frac{2}{\underline{p}} \left[\delta(\sqrt{2}\gamma_n T_n + \gamma_n^2) + 12LK u \right].$$

Then, with probability at least $1 - 2KLe^{-u}$,

$$|\widehat{T}_n - T_n| \leq \frac{2}{\underline{p}} \left[\delta(T_n + \sqrt{nL/2}) + 12Ku\sqrt{L/n} \right]$$

using $\sqrt{nL/2} \leq \gamma_n \leq \sqrt{nL}$ which holds for $L \geq 2$. Assuming $2\delta/\underline{p} \leq 1/2$, we can apply Lemma 8 to get

$$d_K(\widehat{T}_n, Z) \leq d_K(T_n, Z) + \frac{1}{\underline{p}} \left[\delta(1 + \sqrt{nL/2}) + 12Ku\sqrt{L/n} \right] + 2KLe^{-u}.$$

Using $1 + \sqrt{nL/2} \leq 2\sqrt{nL/2}$ and noting that $\delta\sqrt{n} = 2\sqrt{u/\omega_n}$ where $\omega_n = \alpha/n = \min_k \pi_k d_{\text{av}}^{(k)}$, we obtain (44), finishing the proof.

B Proofs of Auxilray Lemmas

B.1 Lemmas in the proof of Theorem 1

To prove Lemma 6, we use the following observation: The central moments of sums of i.i.d. random variables grow “slowly”. To develop an intuition for this observation, recall that

$$\mu_4(X) = \kappa_4(X) + 3\kappa_2^2(X) \quad (50)$$

where X is any random variable, $\mu_r(X)$ is its r th order central moment, and $\kappa_r(X)$ is the corresponding r th order cumulant. Assume that X can be written as a sum of i.i.d. variables $\{Y_1, \dots, Y_n\}$, that is, $X = \sum_{i=1}^n Y_i$. Cumulants are additive over independent sums, hence $\kappa_r(X) = \sum_{i=1}^n \kappa_r(Y_i) = n\kappa_r(Y_1)$. It follows that

$$\mu_4(X) = n\kappa_4(Y_1) + 3n^2\kappa_2^2(Y_1) = O(n^2) \quad (51)$$

assuming $\kappa_r(Y_1) = O(1)$. In other words, $\mu_4(X)$ scales at half the rate of the worst-case scaling of the 4th power of a sum of n deterministic terms (i.e., $O(n^2)$ instead of $O(n^4)$). By using $\kappa_4(Y_1) = \mu_4(Y_1) - 3\kappa_2^2(Y_1)$ and $\kappa_2(Y_1) = \mu_2(Y_1)$, we can express the constants in (51) in terms of the central moments of Y_1 ,

$$\mu_4(X) = n\mu_4(Y_1) + 3n(n-1)\mu_2^2(Y_1) \sim 3\mu_2^2(Y_1)n^2. \quad (52)$$

A similar idea holds for higher-order central moments, an example of which is Lemma 6.

Proof of Lemma 6. Let $\{W'_i\}$ be an independent copy of $\{W_i\}$, and let $X'_n = \sum_{i=1}^n W'_i$. The function $x \mapsto |x|^3$ is convex on \mathbb{R} . Applying Jensen’s inequality with respect to X' and the Cauchy-Schwartz inequality in probability,

$$\mathbb{E}|X_n^2 - \mathbb{E}X_n^2|^3 \leq \mathbb{E}|X_n^2 - (X'_n)^2|^3 \leq [\mathbb{E}|X_n + X'_n|^6]^{1/2} [\mathbb{E}|X_n - X'_n|^6]^{1/2}.$$

For a random variable U , write $\kappa_i(U)$ for its i th cumulant. Then,

$$\begin{aligned} \kappa_i(X_n + X'_n) &= \kappa_i(X_n) + \kappa_i(X'_n) = 2n\kappa_i(W_1), \\ \kappa_i(X_n - X'_n) &= \kappa_i(X_n) + (-1)^i \kappa_i(X'_n) = 2n\kappa_i(W_1) \cdot 1\{\text{is even}\}. \end{aligned}$$

Recall that the 6th central moment μ_6 of any random variable can be written in terms of its cumulants $\{\kappa_i\}$ as follows: $\mu_6 = \kappa_6 + 15\kappa_4\kappa_2 + 10\kappa_3^2 + 15\kappa_2^3$. Writing $\tilde{\kappa}_i = \kappa_i(W_1)$, and applying this relation to $X_n + X'_n$ and $X_n - X'_n$, we have

$$\begin{aligned} \mathbb{E}|X_n + X'_n|^6 &= \mu_6(X_n + X'_n) = 2n\tilde{\kappa}_6 + 60n^2\tilde{\kappa}_4\tilde{\kappa}_2 + 40n^2\tilde{\kappa}_3^2 + 120n^3\tilde{\kappa}_2^3, \\ \mathbb{E}|X_n - X'_n|^6 &= \mu_6(X_n - X'_n) = 2n\tilde{\kappa}_6 + 60n^2\tilde{\kappa}_4\tilde{\kappa}_2 + 120n^3\tilde{\kappa}_2^3. \end{aligned}$$

Let $C_{W_1} = 2|\tilde{\kappa}_6| + 60|\tilde{\kappa}_4|\tilde{\kappa}_2 + 40\tilde{\kappa}_3^2 + 120\tilde{\kappa}_2^3$. Then, $\mathbb{E}|X_n \pm X'_n|^6 \leq C_{W_1}n^3$ and the result follows.

For the case of where $W_1 = \alpha(Z - p)$ where $Z \sim \text{Ber}(p)$, let $\kappa_i = \kappa_i(Z)$ and note that $\tilde{\kappa}_i = \alpha^i \kappa_i$. It follows that

$$C_{W_1} = \alpha^6 (2|\kappa_6| + 60|\kappa_4|\kappa_2 + 40\kappa_3^2 + 120\kappa_2^3).$$

Next, we have $\kappa_2 = p(1-p)$, $\kappa_3 = \kappa_2(1-2p)$, $\kappa_4 = \kappa_2(1-6\kappa_2)$, $\kappa_6 = \kappa_2(1-30\kappa_2(1-4\kappa_2))$. We have $\kappa_2 \in [0, 1/4]$, hence $\kappa_3/\kappa_2 \in [-1, 1]$, $\kappa_4/\kappa_2 \in [-\frac{1}{2}, 1]$ and $\kappa_6/\kappa_2 \in [-\frac{7}{8}, 1]$. It follows that $|\kappa_r| \leq \kappa_2 \leq 1/4$ for all $r = 3, 4, 6$. Then,

$$C_{W_1}/\alpha^6 \leq 2\kappa_2 + 15\kappa_2 + 10\kappa_2 + 7.5\kappa_2 = 34.5\kappa_2$$

and the proof is complete. \square

Proof of Lemma 5. For the expectation, we note that $\mathbb{E}(X_\ell - dp_\ell)^2 = p_\ell(1-p_\ell)$, hence $\mathbb{E}\psi(X_i, dp_\ell) = 1-p_\ell$ and the result follows since $\sum_\ell(1-p_\ell) = L-1$. We now turn to the variance. Let $\tilde{X} = X - dp = \sum_{i=1}^d \tilde{U}_i$, where $\tilde{U}_i = U_i - p$ and $U_i \sim \text{Mult}(1, p)$, independently. We have

$$d^2\mathbb{E}Y^2 = \sum_{\ell=1}^L \frac{\mathbb{E}\tilde{X}_\ell^4}{p_\ell^2} + \sum_{\ell \neq \ell'} \frac{\mathbb{E}\tilde{X}_\ell^2 \tilde{X}_{\ell'}^2}{p_\ell p_{\ell'}}.$$

Noting that $\tilde{X}_\ell = \sum_i \tilde{U}_{i\ell}$, we obtain

$$\mathbb{E}(\tilde{X}_\ell^2 \tilde{X}_{\ell'}^2) = \mathbb{E}\left(\sum_{i_1, i_2} \tilde{U}_{i_1\ell} \tilde{U}_{i_2\ell'}\right)^2 = \sum_{i_1, i_2, i_3, i_4} \mathbb{E}[\tilde{U}_{i_1\ell} \tilde{U}_{i_2\ell} \tilde{U}_{i_3\ell'} \tilde{U}_{i_4\ell'}],$$

where all four indices running from 1 to d . We can categorize the general term $\mathbb{E}[\tilde{U}_{i_1\ell} \tilde{U}_{i_2\ell} \tilde{U}_{i_3\ell'} \tilde{U}_{i_4\ell'}]$ based on how many different values i_1, i_2, i_3 and i_4 take. If i_1, i_2, i_3 and i_4 take 3 or 4 different values, the term is zero by independence. The remaining three cases are summarized below:

$$\mathbb{E}[\tilde{U}_{i_1\ell} \tilde{U}_{i_2\ell} \tilde{U}_{i_3\ell'} \tilde{U}_{i_4\ell'}] = \begin{cases} \mathbb{E}[\tilde{U}_{1\ell}^2] \cdot \mathbb{E}[\tilde{U}_{1\ell'}^2], & i_1 = i_2 \neq i_3 = i_4, \\ (\mathbb{E}[\tilde{U}_{1\ell} \tilde{U}_{1\ell'}])^2, & i_1 = i_3 \neq i_2 = i_4 \text{ or } i_1 = i_4 \neq i_2 = i_3, \\ \mathbb{E}[\tilde{U}_{1\ell}^2 \tilde{U}_{1\ell'}^2], & i_1 = i_3 = i_2 = i_4, \end{cases}$$

which simplifies to

$$\mathbb{E}[\tilde{U}_{i_1\ell} \tilde{U}_{i_2\ell} \tilde{U}_{i_3\ell'} \tilde{U}_{i_4\ell'}] = \begin{cases} p_\ell(1-p_\ell)p_{\ell'}(1-p_{\ell'}), & i_1 = i_2 \neq i_3 = i_4, \\ p_\ell^2 p_{\ell'}^2, & i_1 = i_3 \neq i_2 = i_4 \text{ or } i_1 = i_4 \neq i_2 = i_3, \\ p_\ell p_{\ell'}(p_\ell + p_{\ell'} - 3p_\ell p_{\ell'}), & i_1 = i_3 = i_2 = i_4. \end{cases}$$

The first two cases follow easily from independence. $\mathbb{E}[\tilde{U}_{1\ell}^2] = \text{var}(U_{1\ell}) = p_\ell(1-p_\ell)$ and $\mathbb{E}[\tilde{U}_{1\ell} \tilde{U}_{1\ell'}] = \text{cov}(U_{1\ell}, U_{1\ell'}) = -p_\ell p_{\ell'}$. The third case follows, after some algebra, from the following observation:

$$(\tilde{U}_{1\ell}, \tilde{U}_{1\ell'}) = \begin{cases} (-p_\ell, -p_{\ell'}) & \text{w.p. } 1 - (p_\ell + p_{\ell'}) \\ (-p_\ell, 1 - p_{\ell'}) & \text{w.p. } p_{\ell'} \\ (1 - p_\ell, -p_{\ell'}) & \text{w.p. } p_\ell \end{cases}.$$

To sum up, for $\ell \neq \ell'$, we have

$$\begin{aligned} \mathbb{E}[\tilde{X}_\ell^2 \tilde{X}_{\ell'}^2] &= (d^2 - d)p_\ell p_{\ell'}[(1-p_\ell)(1-p_{\ell'}) + 2p_\ell p_{\ell'}] + dp_\ell p_{\ell'}(p_\ell + p_{\ell'} - 3p_\ell p_{\ell'}) \\ &= dp_\ell p_{\ell'}[(d-1) + (2-d)(p_\ell + p_{\ell'}) + (3d-6)p_\ell p_{\ell'}]. \end{aligned}$$

Let $\alpha := \sum_{\ell} p_{\ell}^2$. Using $\sum_{\ell \neq \ell'} p_{\ell} p_{\ell'} = 1 - \alpha$ and $\sum_{\ell \neq \ell'} p_{\ell} = \sum_{\ell \neq \ell'} p_{\ell'} = L - 1$, we have

$$\frac{1}{d} \sum_{\ell \neq \ell'} \frac{\mathbb{E}[\tilde{X}_{\ell}^2 \tilde{X}_{\ell'}^2]}{p_{\ell} p_{\ell'}} = (d-1)(L^2 - L) + 2(2-d)(L-1) + (3d-6)(1-\alpha),$$

for $\ell \neq \ell'$. Next, we consider the case $\ell = \ell'$. Let κ_n and μ_n denote n th order cumulants and central moments of $\tilde{U}_{1\ell}$. By (52),

$$\begin{aligned} \mathbb{E}[\tilde{X}_{\ell}^4] &= d\mu_4 + 3d(d-1)\mu_2^2 \\ &= d[p_{\ell}(1-p_{\ell})^4 + p_{\ell}^4(1-p_{\ell})] + 3d(d-1)p_{\ell}^2(1-p_{\ell})^2 \\ &= dp_{\ell}^2[1/p_{\ell} + (3d-7) + (12-6d)p_{\ell} + (3d-6)p_{\ell}^2]. \end{aligned}$$

We obtain

$$\frac{1}{d} \sum_{\ell=1}^L \frac{\mathbb{E}\tilde{X}_{\ell}^4}{p_{\ell}^2} = \frac{L}{h(p)} + L(3d-7) + (12-6d) + (3d-6)\alpha.$$

Putting the pieces together, we have

$$d\mathbb{E}Y^2 = d(L^2 - 1) + \frac{L}{h(p)} - L(L+2) + 2.$$

Combining with $\text{var}(Y) = \mathbb{E}Y^2 - (L-1)^2$ and some algebra finishes the proof. \square

Proof of Lemma 7. We have $\sum_i d_i(x_i - y - v)^2 = \sum_i d_i(x_i - y)^2 - 2vR + d_+v^2$. Hence,

$$\sum_i d_i \psi(x_i, y + v) = \frac{\sum_i d_i(x_i - y)^2}{y + v} - \frac{2v}{y + v}R + \frac{v^2}{y + v}d_+.$$

It follows, after some algebra, that

$$\sum_i d_i[\psi(x_i, y + v) - \psi(x_i, y)] = -\frac{v}{y + v} \left[\sum_i d_i \psi(x_i, y) + 2R - vd_+ \right].$$

We obtain

$$|G(v) - G(0)| \leq \frac{|v|}{|y + v|} [G(0) + 2|R| + |v|d_+].$$

Applying the inequality $|a|/|1+a| \leq 2|a|$ which holds for any $|a| \leq 1/2$, with $a = v/y$ finishes the proof. \square

To prove Lemma 8, we first need an auxiliary lemma.

Lemma 9. *Let $T = \beta S + \alpha$ where S is random variable and $\beta, \alpha \in \mathbb{R}$ are constants, and let $Z \sim N(0, 1)$. Then,*

$$d_K(T, Z) \leq d_K(S, Z) + \frac{|\beta - 1|}{\sqrt{2\pi e} \min\{|\beta|, 1\}} + \frac{|\alpha|}{\sqrt{2\pi}}.$$

Proof of Lemma 9. We have

$$\begin{aligned}
d_K(T, Z) &= \sup_{t \in \mathbb{R}} |\mathbb{P}(\beta S + \alpha \leq t) - \Phi(t)| \\
&= \sup_{t \in \mathbb{R}} |\mathbb{P}(S \leq t) - \Phi(\beta t + \alpha)| \\
&\leq \sup_{t \in \mathbb{R}} (|\mathbb{P}(S \leq t) - \Phi(t)| + |\Phi(t) - \Phi(\beta t + \alpha)|) \\
&= d_K(S, Z) + \sup_{t \in \mathbb{R}} |\Phi(t) - \Phi(\beta t + \alpha)|.
\end{aligned}$$

Then,

$$\begin{aligned}
|\Phi(t) - \Phi(\beta t)| &= \left| \int_{\beta t}^t \frac{1}{\sqrt{2\pi}} e^{-x^2/2} dx \right| \\
&\leq |\beta t - t| \frac{1}{\sqrt{2\pi}} e^{-\min(t, \beta t)^2/2} = \frac{1}{\sqrt{2\pi}} |\beta - 1| \cdot |t| e^{-at^2/2},
\end{aligned}$$

where $a = \min(\beta^2, 1)$. Note that $t \mapsto t e^{-at^2/2}$ achieves its maximum of $1/\sqrt{ae}$ over $[0, \infty)$ at $t = 1/\sqrt{a}$. We also have $|\Phi(s) - \Phi(s + \alpha)| \leq |\alpha| \sup_{\tilde{s}} \Phi'(\tilde{s}) = \frac{1}{\sqrt{2\pi}} |\alpha|$. Putting the pieces together finishes the proof. \square

Proof of Lemma 8. Let $\mathcal{A} = \{|\widehat{T}_n - T_n| \geq \delta T_n + \varepsilon\}$ and $q = \mathbb{P}(\mathcal{A})$. For any $t \in \mathbb{R}$, we have

$$\begin{aligned}
\mathbb{P}(\widehat{T}_n \leq t) &\leq \mathbb{P}(\{\widehat{T}_n \leq t\} \cap \mathcal{A}^c) + \mathbb{P}(\mathcal{A}) \\
&\leq \mathbb{P}((1 - \delta)T_n - \varepsilon \leq t) + q.
\end{aligned}$$

Subtracting $\Phi(t) = \mathbb{P}(Z \leq t)$ from both sides, we get

$$\begin{aligned}
\mathbb{P}(\widehat{T}_n \leq t) - \Phi(t) &\leq d_K((1 - \delta)T_n - \varepsilon, Z) + q \\
&\leq d_K(T_n, Z) + \frac{2\delta}{\sqrt{2\pi}e} + \frac{\varepsilon}{\sqrt{2\pi}} + q \leq d_K(T_n, Z) + \frac{1}{2}(\delta + \varepsilon) + q,
\end{aligned}$$

by Lemma 9 and noting that $\min\{|1 - \delta|, 1\} \geq 1/2$ by assumption. Similarly, for any $s \in \mathbb{R}$,

$$\begin{aligned}
\mathbb{P}(T_n \leq s) &\leq \mathbb{P}(\{T_n \leq s\} \cap \mathcal{A}^c) + \mathbb{P}(\mathcal{A}) \\
&\leq \mathbb{P}(\widehat{T}_n \leq (1 + \delta)s + \varepsilon) + q.
\end{aligned}$$

Applying the change of variable $t = (1 + \delta)s + \varepsilon$, adding Φ and rearranging, we obtain

$$\Phi(t) - \mathbb{P}(\widehat{T}_n \leq t) \leq \Phi(t) - \mathbb{P}((1 + \delta)T_n + \varepsilon \leq t) + q,$$

and the rest of the argument follows as in the previous case. Putting the pieces together finishes the proof. \square

B.2 Lemmas in the proofs of Section 6

The following proposition, controlling the tail probability of a randomly-selected Poisson sum, is used in the proof of Lemma 1:

Proposition 3. Let $A_j \sim \text{Poi}(\lambda_j)$ and $U_j \sim \text{Ber}(1/2)$ for $j = 1, \dots, n$, and assume that $\{A_j, U_j, j = 1, \dots, n\}$ are independent. Let $d = \sum_{j=1}^n A_j U_j$ and $d^* = \mathbb{E}[d]$. Then,

$$\mathbb{P}(|d - d^*| \geq d^*/2) \leq 2e^{-0.008d^*} + 4e^{-0.03d^*/\lambda_{\max}}$$

where $\lambda_{\max} = \max_j \lambda_j$.

Proof of Proposition 3. Let $\tilde{d} = \sum_j \lambda_j U_j$ and $d^* = \frac{1}{2} \sum_j \lambda_j$, so that $d^* = \mathbb{E}[\tilde{d}]$. Conditioned on $U = (U_1, \dots, U_n)$, d is a Poisson variable with mean \tilde{d} . If $X \sim \text{Poi}(\lambda)$, then for any $t \in (0, 1]$, we have $\mathbb{P}(|X - \lambda| \geq t\lambda) \leq 2 \exp(-\lambda t^2/4)$; see Lemma 12 (Section C). Then,

$$\mathbb{P}(|d - \tilde{d}| \geq 0.2\tilde{d} \mid U) \leq 2 \exp(-0.01\tilde{d}).$$

Next, we apply Proposition 4 (Section C) to $\tilde{d} - d^* = \sum_j \lambda_j (U_j - 1/2)$. Since $|\lambda_j (U_j - 1/2)| \leq \lambda_{\max}$ and $\text{var}(\tilde{d} - d^*) = \sum_j \lambda_j^2/4 \leq \lambda_{\max}(d^*/2)$, we have

$$\mathbb{P}(|\tilde{d} - d^*| \geq \sqrt{\lambda_{\max} d^* u} + \lambda_{\max} u/3) \leq 2e^{-u}.$$

Taking $u = 0.03d^*/\lambda_{\max}$, we obtain $\mathbb{P}(|\tilde{d} - d^*| \geq 0.2d^*) \leq 2 \exp(-0.03d^*/\lambda_{\max})$.

Let $\mathcal{A} = \{|d - \tilde{d}| \geq 0.2\tilde{d}\}$ and $\mathcal{B} = \{|\tilde{d} - d^*| \geq 0.2d^*\}$. Note that \mathcal{B} is completely determined by U . On $\mathcal{A}^c \cap \mathcal{B}^c$, we have $(0.8)^2 d^* < d < (1.2)^2 d^*$, implying $|d - d^*| < d^*/2$. It follows that

$$\mathbb{P}(|d - d^*| \geq d^*/2) \leq \mathbb{P}(\mathcal{A} \cup \mathcal{B}) \leq \mathbb{P}(\mathcal{A}) + \mathbb{P}(\mathcal{B}).$$

We have $\mathbb{P}(\mathcal{A}) = \mathbb{E}[\mathbb{P}(\mathcal{A} \mid U) 1_{\mathcal{B}^c} + \mathbb{P}(\mathcal{A} \mid U) 1_{\mathcal{B}}]$, hence

$$\begin{aligned} \mathbb{P}(\mathcal{A}) &\leq \mathbb{E}[\mathbb{P}(\mathcal{A} \mid U) 1_{\mathcal{B}^c} + 1_{\mathcal{B}}] \\ &\leq 2\mathbb{E}[e^{-0.01\tilde{d}} 1_{\mathcal{B}^c}] + \mathbb{P}(\mathcal{B}) \\ &\leq 2e^{-0.008d^*} \mathbb{E}[1_{\mathcal{B}^c}] + \mathbb{P}(\mathcal{B}) \end{aligned}$$

using $\tilde{d} \geq 0.8d^*$ on \mathcal{B}^c . We further bound $\mathbb{E}[1_{\mathcal{B}^c}] \leq 1$. Putting the pieces together finishes the proof. \square

Proof of Lemma 1. Recall that $d_i = \sum_{j=1}^n A_{ij} U_j$ where $\{U_j = 1\{j \in S_1\}\}$ is an independent $\text{Ber}(1/2)$ sequence, and $d_i^* = \mathbb{E}[d_i]$. We also recall from (32) that $d_i^* \geq \frac{1}{2} C_1 \nu_n$ for all $i \in [n]$. Fix $i \in [n]$. We apply Proposition 3 to d_i with $\lambda_j = \mathbb{E}[A_{ij}] = (\nu_n/n) \theta_i \theta_j B_{z_i z_j}^0$. Since $\|B^0\|_\infty = 1$ and $\theta_{\max} = 1$, we have $\max_j \lambda_j \leq \nu_n/n$, and thus

$$\frac{d_i^*}{\max_j \lambda_j} \geq \frac{C_1}{2} n \geq \frac{200}{3} \log n,$$

where the first inequality is by (32) and the second by assumption (23). Proposition 3 gives

$$\mathbb{P}(|d_i - d_i^*| \geq d_i^*/2) \leq 2e^{-0.004C_1 \nu_n/2} + 4e^{-2 \log n} \leq 6n^{-2}$$

since $0.004C_1 \nu_n/2 \geq 2 \log n$ by assumption (23). By union bound,

$$\mathbb{P}(d_i \notin [\frac{1}{2}d_i^*, \frac{3}{2}d_i^*] \text{ for some } i \in [n]) \leq 6n^{-1}. \quad (53)$$

Furthermore, $\tilde{n}_k := |\mathcal{G}_k| = n_k - |\mathcal{C}_k \cap S_1| = n_k - \sum_{i \in \mathcal{C}_k} U_i$ for all k . Applying Proposition 4 (Section C) with $u = 0.01n_k$, we obtain

$$\left| \frac{\tilde{n}_k}{n_k} - \frac{1}{2} \right| = \left| \frac{1}{n_k} \sum_{i \in \mathcal{C}_k} U_i - \frac{1}{2} \right| \geq \sqrt{0.01} + \frac{0.01}{3} \geq 0.1$$

with probability $\leq 2e^{-0.01n_k}$. By union bound

$$\mathbb{P}(\tilde{n}_k \notin [0.4n_k, 0.6n_k] \text{ for some } k \in [K_0]) \leq 2 \sum_{k=1}^{K_0} e^{-0.01n_k} \leq 2K_0 e^{-0.01\tau_C n} \leq n^{-1}. \quad (54)$$

The last inequality is since assumption (23) implies $0.01\tau_C n \geq \log(n^3) \geq \log(2K_0 n)$. The result follows by combining (53) and (54). \square

B.2.1 Lemmas in the proof of Theorem 2

Proof of Lemma 2. Let $U_t := \mathbb{P}(Y \leq t \mid \mathcal{F})$ and set $U = (U_t, t \in \mathbb{R})$ and $b_t = \mathbb{P}(Z \leq t)$. The function $f(U) = \sup_{t \in \mathbb{R}} |U_t - b_t|$ is convex, hence by Jensen's inequality

$$d_K(Y, Z) = f(\mathbb{E}U) \leq \mathbb{E}f(U) = \mathbb{E}[d_K(\mathcal{L}(Y \mid \mathcal{F}), Z)].$$

Next, letting $Y' := Y1_{\mathcal{B}}$, we have

$$\begin{aligned} \mathbb{P}(Y' \leq t) &\leq \mathbb{P}(\{Y' \leq t\} \cap \mathcal{B}) + \mathbb{P}(\mathcal{B}^c) \\ &= \mathbb{P}(\{Y \leq t\} \cap \mathcal{B}) + \mathbb{P}(\mathcal{B}^c) \leq \mathbb{P}(Y \leq t) + \mathbb{P}(\mathcal{B}^c) \end{aligned}$$

and

$$\mathbb{P}(Y' \leq t) \geq \mathbb{P}(\{Y' \leq t\} \cap \mathcal{B}) = \mathbb{P}(\{Y \leq t\} \cap \mathcal{B}) \geq \mathbb{P}(Y \leq t) - \mathbb{P}(\mathcal{B}^c).$$

It follows that $|\mathbb{P}(Y' \leq t) - \mathbb{P}(Y \leq t)| \leq \mathbb{P}(\mathcal{B}^c)$ for all $t \in \mathbb{R}$. An application of the triangle inequality gives $|d_K(Y, Z) - d_K(Y', Z)| \leq \mathbb{P}(\mathcal{B}^c)$ finishing the proof. \square

B.2.2 Lemmas in the proof of Theorem 3

Proof of Lemma 3. Recall that for $i \in \hat{\mathcal{T}}_r$, we have $d_i \xi_{i\ell} \sim \text{Bin}(d_i, q_{r\ell})$, conditioned on \mathcal{F} . Thus, we can write $d_i(\xi_{i\ell} - q_{r\ell}) = \sum_{j=1}^{d_i} Z_j$ where Z_j are centered Bernoulli variables with parameter $q_{r\ell}$. Applying Proposition 4 (Appendix C), we have

$$\mathbb{P}^{\mathcal{F}} \left(\left| \sum_j Z_j \right| \geq \sqrt{2vu} + \frac{u}{3} \right) \leq 2e^{-u}, \quad u \geq 0,$$

where $v = \sum_j \text{var}(Z_j)$. Since, $v = d_i q_{r\ell}(1 - q_{r\ell}) \leq d_i/4$, taking $u = 2 \log n$, we have

$$\mathbb{P}^{\mathcal{F}} \left(|\xi_{i\ell} - q_{r\ell}| \geq \sqrt{\frac{\log n}{d_i}} + \frac{2 \log n}{3d_i} \right) \leq 2n^{-2}.$$

On event \mathcal{A} , we have $d_i \geq d_i^*/2 \geq C_1\nu_n/4$ for all i , by (32). By assumption, $4 \log n \leq C_1\nu_n$, hence on \mathcal{A} ,

$$\sqrt{\frac{\log n}{d_i}} + \frac{2 \log n}{3d_i} \leq 4\sqrt{\frac{\log n}{C_1\nu_n}} = \varepsilon_n.$$

We have $\mathcal{E}^c = \{\max_{r,\ell} \max_{i \in \hat{\mathcal{T}}_r} |\xi_{i\ell} - q_{r\ell}| \geq \varepsilon_n\}$. Using $|\bigcup_r \hat{\mathcal{T}}_r| = |\hat{\mathcal{G}}_k| \leq n$ and the union bound, we obtain $\mathbb{P}^{\mathcal{F}}(\mathcal{E}^c \cap \mathcal{A}) \leq 2(nL) \cdot n^{-2} = 2Ln^{-1}$. The lemma follows by taking the expectation of both sides and using the smoothing property of conditional expectation. \square

Lemma 4 follows from the following more refined result:

Lemma 10. *Let $\psi(x, y) = (x - y)^2/y$. For all (x, y) and (x', y') in $[0, 1] \times [1/c_1, 1]$, where $c_1 > 1$, we have*

$$|\psi(x', y') - \psi(x, y)| \leq c_2|x - y| \cdot \|\delta\| + c_3\|\delta\|^2 \quad (55)$$

where $\delta = (x - x', y - y')$, $c_2 = c_1\sqrt{4 + (1 + c_1)^2}$ and $c_3 = 4c_1^3$.

Assuming that $|x - x'| \leq \varepsilon$ and $|y - y'| \leq \varepsilon$, so that $\|\delta\| \leq \sqrt{2}\varepsilon$, and using $|x - y| \leq 1$,

$$|\psi(x', y') - \psi(x, y)| \leq \sqrt{2}c_2\varepsilon + 2c_3\varepsilon^2 \leq c_4 \max(\varepsilon, \varepsilon^2) \quad (56)$$

where $c_4 = \sqrt{2}c_2 + 2c_3$. Since $c_2 \leq \sqrt{8}c_1^2$, we have $c_4 \leq 12c_1^3$ and Lemma 4 follows.

Proof of Lemma 10. The function ψ is continuously differentiable of all orders, on $\mathbb{R} \times \mathbb{R}_{++}$, with the gradient and Hessian given by

$$\nabla\psi(x, y) = (x/y - 1) \begin{bmatrix} 2 \\ -(1 + x/y) \end{bmatrix}, \quad \nabla^2\psi(x, y) = (2/y) \begin{bmatrix} 1 & -x/y \\ -x/y & x^2/y^2 \end{bmatrix}.$$

The Hessian has eigenvalues 0 and $2(x^2 + y^2)/y^3$. By Taylor expansion,

$$\psi(x', y') - \psi(x, y) = \langle \nabla\psi(x, y), \delta \rangle + \frac{1}{2} \langle \delta, \nabla^2\psi(\tilde{x}, \tilde{y}), \delta \rangle$$

where (\tilde{x}, \tilde{y}) is a point between (x, y) and (x', y') . Since $0 \leq \nabla^2\psi(\tilde{x}, \tilde{y}) \preceq 2(\tilde{x}^2 + \tilde{y}^2)/\tilde{y}^3 I_2$ and $\tilde{y} \geq \min\{y, y'\} \geq 1/c_1$, we obtain

$$|\langle \delta, \nabla^2\psi(\tilde{x}, \tilde{y}), \delta \rangle| \leq \frac{2(\tilde{x}^2 + \tilde{y}^2)}{\tilde{y}^3} \|\delta\|^2 \leq 4c_1^3 \|\delta\|^2.$$

We also have

$$|\langle \nabla\psi(x, y), \delta \rangle| \leq |x/y - 1| \sqrt{4 + (1 + x/y)^2} \|\delta\| \leq c_2 \|\delta\|$$

using the assumption on the ranges of x and y . The result follows. \square

C Other technical results

Lemma 11. *Assume that Z is a random variable taking values z_1, \dots, z_R with probabilities $\hat{\beta}_1, \dots, \hat{\beta}_R$ respectively. Then, $\text{var}(Z) \geq \frac{1}{2}\hat{\beta}_1\hat{\beta}_2(z_1 - z_2)^2$.*

Proof. Let Z' be an independent copy of Z . Then $\text{var}(Z) = \frac{1}{2}\mathbb{E}(Z - Z')^2$, and (Z, Z') takes value (z_1, z_2) with probability $\hat{\beta}_1\hat{\beta}_2$. The result follows. \square

Lemma 12. *Let $X \sim \text{Poi}(\lambda)$. Then, for any $t \in (0, 1]$,*

$$\mathbb{P}(|X - \lambda| \geq t\lambda) \leq 2 \exp(-\lambda t^2/4).$$

Proof of Lemma 12. Fix $t \in (0, 1]$. For $\theta \in (0, 1.79]$, by the Chernoff bound,

$$\mathbb{P}(X - \lambda \geq t\lambda) \leq e^{-\theta t\lambda} \mathbb{E}[e^{(X-\lambda)\theta}] = e^{-\theta t\lambda} \exp(\lambda(e^\theta - 1 - \theta)) \leq e^{\lambda\theta^2 - \theta t\lambda}$$

using $e^\theta - 1 - \theta \leq \theta^2$ when $\theta \leq 1.79$. Since $\lambda\theta^2 - \theta t\lambda$ attains its minimum at $\theta = t/2 \leq 1$, we obtain $\mathbb{P}(X - \lambda \geq t\lambda) \leq \exp(-\lambda t^2/4)$. On the other hand,

$$\mathbb{P}(\lambda - X \geq t\lambda) \leq e^{-\theta t\lambda} \mathbb{E}[e^{(\lambda-X)\theta}] = e^{-\theta t\lambda} \exp(\lambda(e^{-\theta} - 1 + \theta)) \leq e^{\lambda\theta^2/2 - \theta t\lambda}$$

using $e^{-\theta} - 1 + \theta \leq \theta^2/2$ for $\theta \geq 0$. Since $\lambda\theta^2/2 - \theta t\lambda$ attains its smallest value at $\theta = t \leq 1$, we get $\mathbb{P}(\lambda - X \geq t\lambda) \leq \exp(-\lambda t^2/2)$, finishing the proof. \square

Proposition 4 (Giné and Nickl [GN15] Theorem 3.1.7). *Let $S = \sum_{i=1}^n X_i$ where $\{X_i\}$ are independent random variables with $|X_i - \mathbb{E}X_i| \leq c$ for all i . Let $v \geq \text{var}(S)$. Then, for all $u \geq 0$,*

$$\mathbb{P}\left(|S - \mathbb{E}S| \geq \sqrt{2vu} + \frac{cu}{3}\right) \leq 2e^{-u}.$$

In particular, if $S \sim \text{Bin}(n, p)$, then we can take $v = \mathbb{E}[S] \geq \text{var}(S)$. Letting $\hat{p} = S/n$, the result gives $\mathbb{P}(|\hat{p} - p| \geq \sqrt{\frac{2pu}{n}} + \frac{u}{3n}) \leq 2e^{-u}$.

D Extra simulations

D.1 Model Selection

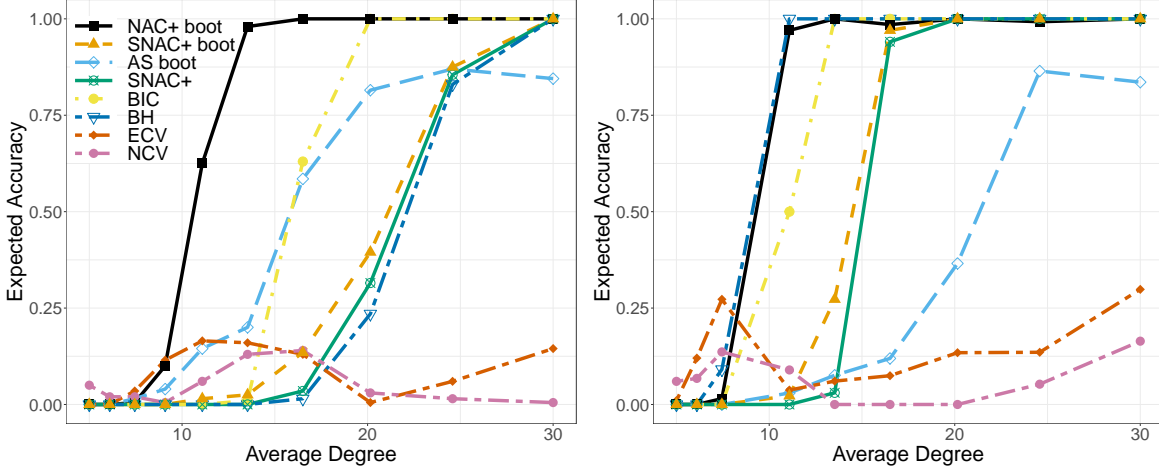


Figure 8: Expected accuracy of selecting the true number of communities versus expected average degree of the network. The data follows a DCSBM with $n = 5000$, $\beta = 0.2$, $\theta_i \sim \text{Pareto}(3/4, 4)$, and connectivity matrix B_3 . Left plot has unbalanced community sizes proportional to $(1, 1, 2, 3)$ and the right plot has balanced community sizes.

Figure 8 shows the model selection accuracy under similar setting to Section 5.2.1 but with a generalized version of B_1 as the connectivity matrix, given by

$$B_3 \propto (1 - \beta) \text{diag}(w) + \beta \mathbf{1}\mathbf{1}^T.$$

It is evident that B_1 is a special case of B_3 where w is the an all-ones vector. Here, we set $w = (1, 2, 3, 1)$ under $K = 4$, while other parameters stay the same as in Section 5.2.1: $n = 5000$, $\beta = 0.2$ and $\theta_i \sim \text{Pareto}(3/4, 4)$. The left plot in Figure 8 shows the case where the DCSBM has unbalanced community sizes proportional to $(1, 1, 2, 3)$ and the right plot shows balanced community sizes. All methods have lower accuracy in the unbalanced setting except for the AS. BH is affected the most while NAC+ the least. The robustness of NAC+ could be because its performance mainly relies on the full version of ρ and unbalanced sizes retain its rows' distinction. However, the SNAC+ is still affected by the unbalanced community sizes because of the increased difficulty in recovering the correct labels and the increased variance in ρ due to subsampling.

D.2 ROC curves

We consider additional testing with $H_0 : K = 4$ vs. $H_a : K = 3$. Other DCSBM simulating parameters are the same as in Section 5.2.2. Figure 9 shows ROC curves for the null being DCSBM with $K = 4$ and two alternatives: a DCSBM with $K = 3$ (left) and a DCLVM with $K = 3$ (right). In addition, we also have $n = 2000$ for the upper row and $n = 10000$ for the lower. Similar to Figure 2, the performance of the tests get better as n increases. NAC and AS tests are nearly perfect (achieve 100% recovery for very small type I error) when the

alternative is DCLVM. The LR test is almost perfect in distinguishing two DCSBMs but has very poor power when the alternative is DCLVM.

We also include the test $H_0 : K = 4$, DCSBM vs. $H_a : K = 4$, DCLVM with similar parameters in Figure 10. It shows that NAC tests are still able to reject when the true model is a DCLVM with the same number of communities as the DCSBM. Note that we have excluded the LR test in this case, since it is the likelihood ratio of two fitted DCSBMs with different number of communities, but here we have models with the same number of communities.

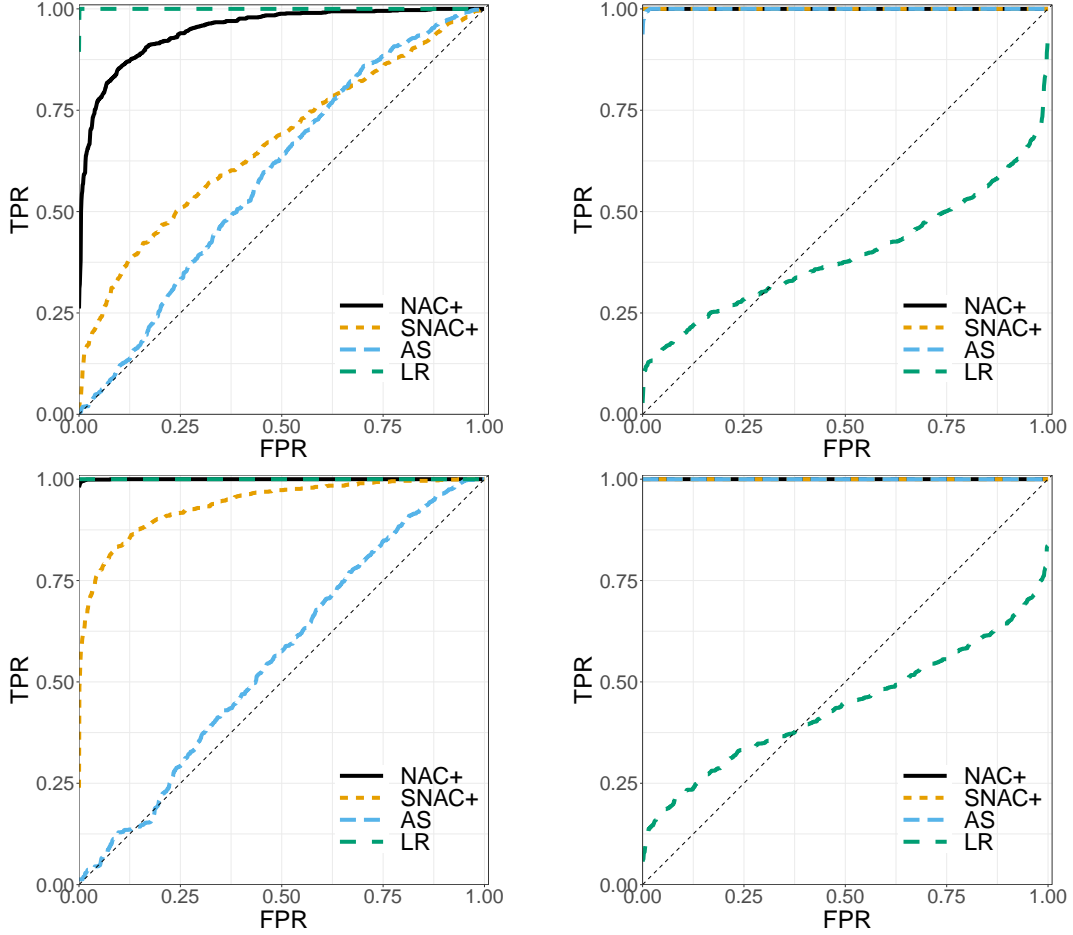


Figure 9: ROC plots for testing 4- versus 3-community models. Top and bottom rows correspond to $n = 2000$ and $n = 10000$, respectively. Left and right columns correspond to the DCSBM and DCLVM alternatives, respectively.

D.3 More real network examples

Figure 11 and 12 provide more profile plots for the networks in the FB-100 dataset. The former collection shows profile plots with one-elbow pattern and the latter shows higher variability of SNAC+ statistics with multi-stage elbows/dips. We also point out that the Caltech network in Figure 12 is the only FB-100 network for which SNAC+ drops to nearly zero (at $K = 10$) within the range of candidate K . However, the statistic continues to decrease afterwards and

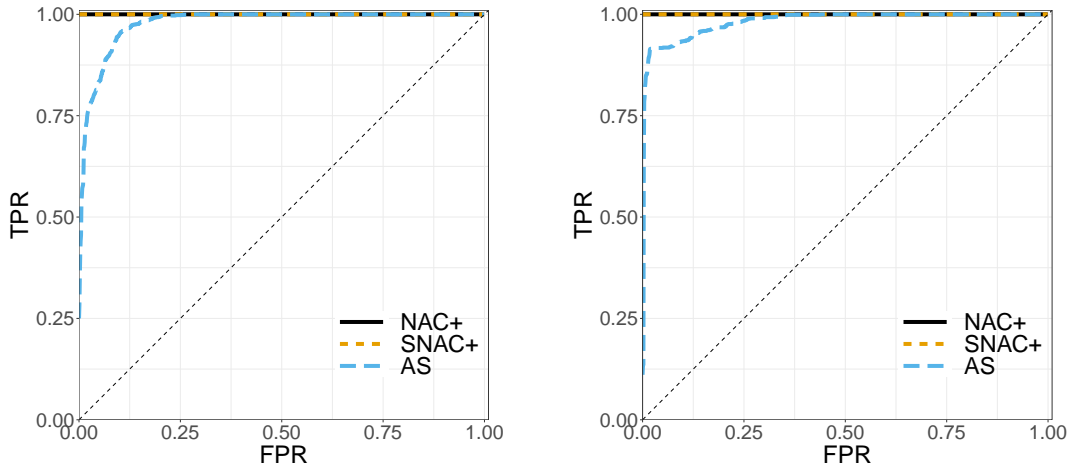


Figure 10: ROC plots for testing $H_0 : K = 4$ DCSBM vs. $H_a : K = 4$ DCLVM. Left has $n = 2000$ and right $n = 10000$.

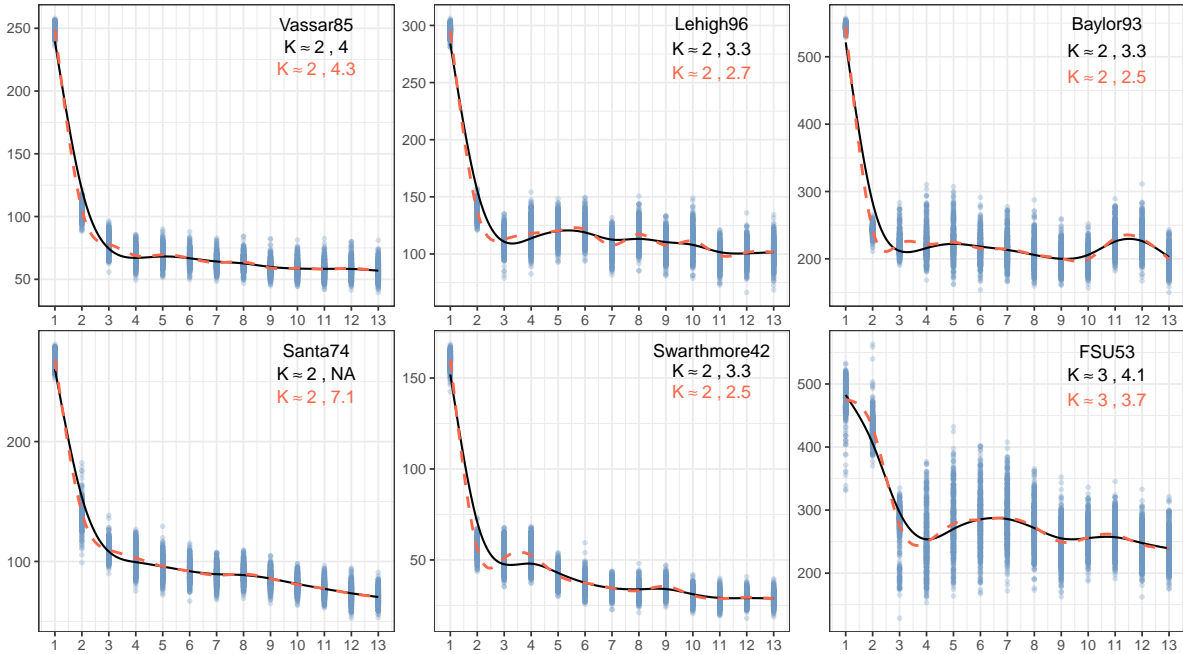


Figure 11: More examples on community profile plots from FB-100. They show a single elbow/dip pattern.

does not show any dips/elbows like others. This suggests that although we cannot reject the null hypothesis of a DCSBM (with $K = 10$) in this case, a DCSBM still might not be a good model for the network. That we cannot reject the null for this case is most likely due to the small community sizes we get with $K = 10$, leading to an insufficient signal.

Figure 13 shows the profile plot for the political blog network and its community structure. In the profile plot, the elbow point identified by the largest second derivative is at $K = 2$, matching the presumed ground truth number of communities in this case. The colored

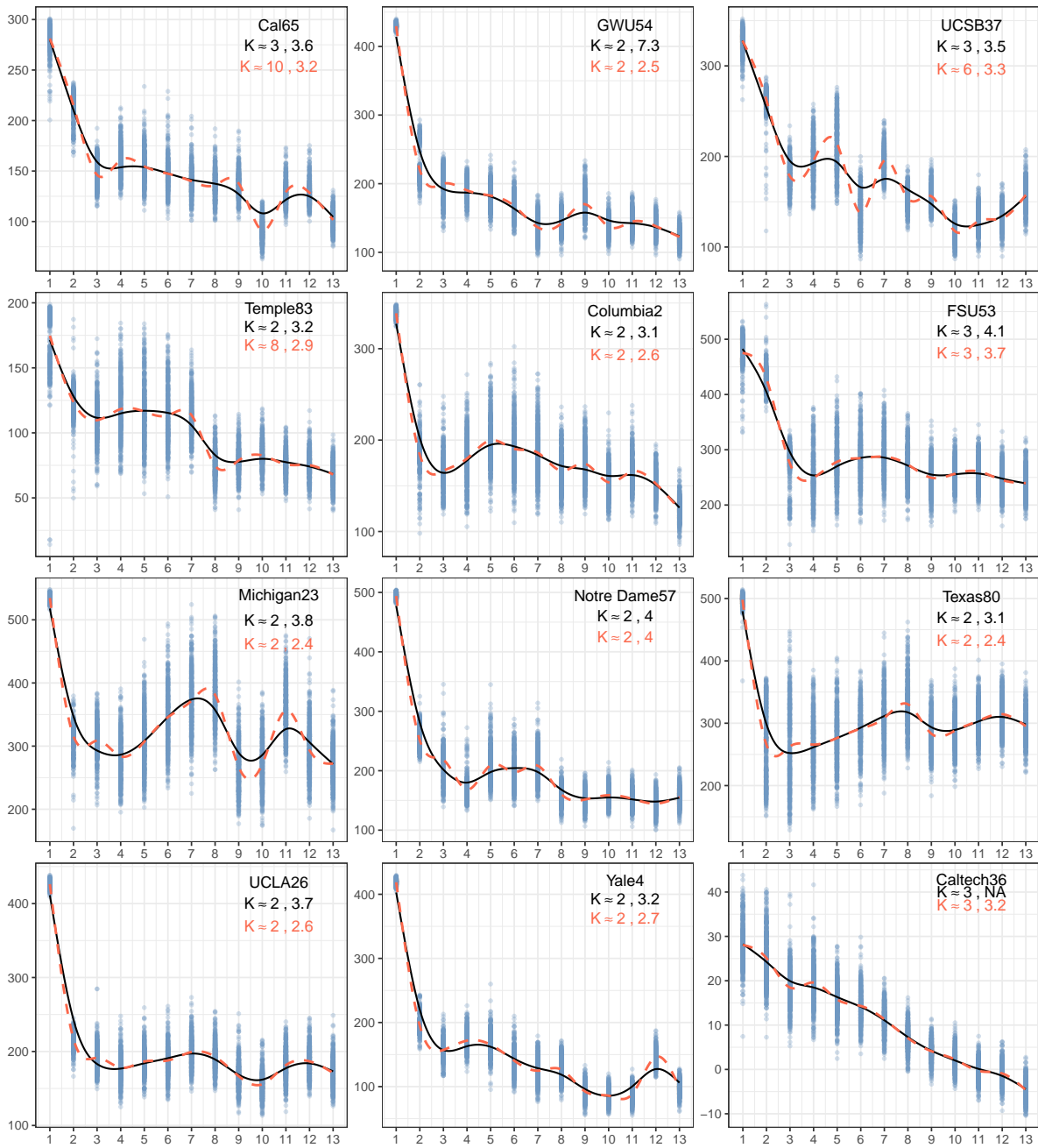


Figure 12: More examples on community profile plots from FB-100. They show a multiple elbows/dips pattern.

community structure also shows that the fitted two-community model gives a reasonable split of the nodes.

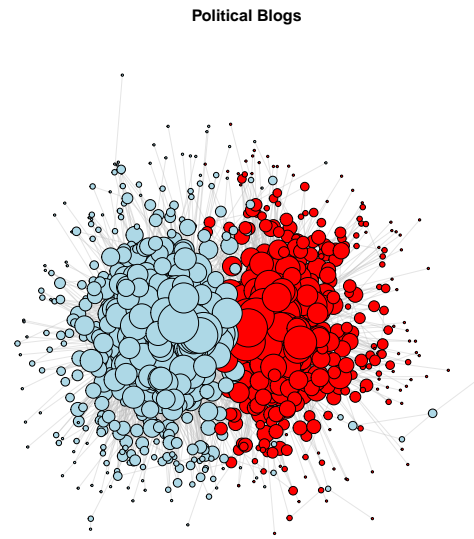
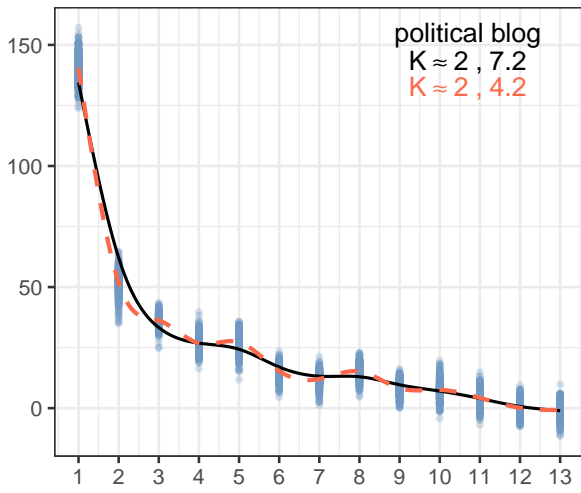


Figure 13: Political blog network: profile plot (left) and community structure (right)